Figure 7 ChEI restores neurogenesis in the DG and OB of mice exposed to chronic restraint. (A) The experimental procedure for the study of the effect of ChEI-treatment on mice exposed to chronic restraint. Following 1 week of administration of saline to habituate the mice to intraperitoneal injections, the animals were divided into three groups; during the week following saline administration, mice were injected with BrdU twice with a 2 h-interval. Subsequently, the mice in the control group (Cont) were left in their home cages without treatment for 4 weeks, while in the restraint group (Rest), mice were restrained for 6 h every day for 4 weeks. In the restraint group with ChEI-treatment (ChEI), mice were pretreated with ChEI (donepezil, 1.0 mg/weight (kg)/day), followed by BrdU injection as described above, and then restrained for 4 weeks. (B) Corticosterone levels in plasma samples taken before restraint on the final day of the experiments. There is no significant difference in plasma corticosterone levels between the groups ($P > 0.05$). (C) The number of Ki67-positive proliferating cells in the DG was significantly decreased by chronic restraint but was not affected by ChEI-treatment ($P = 0.0009$). (D) The numbers of Ki67-positive cells in the SVZ (left), RMS (middle) and OB (right). None of the regions examined showed any significant difference in the number of Ki67-positive cells between the groups ($P > 0.05$). (E–L) Double immunofluorescence for BrdU (red) and NeuN (green) in the DG (E, Cont; F, Rest; G, ChEI) and OB (I, Cont; J, Rest; K, ChEI). Chronic restraint significantly decreased the number of newborn neurons labeled with BrdU in the DG (H, upper) and OB (L, upper). The decrease in neurogenesis was completely reversed by chronic ChEI-treatment (DG, $P = 0.0029$; OB, $P = 0.0161$). The proportions of NeuN-positive neurons in the BrdU-positive cell population in the DG (H, lower) and OB (L, lower) were not affected by either restraint or ChEI-treatment ($P > 0.05$). Scale bars = 100 μm.

4 weeks of restraint stress decreased Ki67-positive proliferating cells in the DG (Fig. 7C, $P = 0.0009$), but not the SVZ, RMS or OB (Fig. 7D, $P > 0.05$). The ChEI-treatment did not affect the number of Ki67-positive cells (Fig. 7C,D). The number of BrdU+NeuN+ newborn neurons in the DG and OB were decreased by restraint stress, indicating that stress reduces the survival of young neurons. However, ChEI-treatment almost completely reversed the suppressive effect of stress on neuronal survival (Fig. 7E–L) (DG, $P = 0.0029$, OB, $P = 0.0161$). There was no significant difference in the percentages of NeuN+ neurons in the BrdU+ cell population between these groups ($P > 0.05$) (Fig. 7H,L). Taken together, these data indicate that chronic ChEI-treatment reverses the stress-induced decrease in the survival of newborn cells, while having no effect on proliferation.

Discussion

Previous studies have indicated that approximately half of newborn neurons die before reaching maturity in the DG and OB (Petreanu & Alvarez-Buylla 2002; Dayer et al. 2003), but the mechanisms regulating the apoptosis of these neurons are largely unknown. Herein, we report that the cholinergic system promotes the survival of newborn neurons in the DG and OB. Cholinergic neurons innervating the DG and OB play an important role in learning and memory formation (Wenk et al. 1977; Zaborszky et al. 1986; McGurk et al. 1991; Leanza et al. 1995). Alterations in these processes affect neurogenesis in the DG and OB (Gould et al. 1999; Gheusi et al. 2000; Shors et al. 2001; Rochefort et al. 2002; Madsen et al. 2003), raising the possibility that the cholinergic system may act on neurogenesis directly and/or indirectly. An indirect effect of cholinergic input on neurogenesis has been proposed based on the observation that lesions in the BFC system reduce expression of brain-derived neurotrophic factor (BDNF) (Hefti 1986; Williams et al. 1986; Berchtold et al. 2002), which promotes neurogenesis (Zigova et al. 1998; Lee et al. 2002). Our results indicate that immature neurons in the adult mouse DG and OB express various ACh receptor subtypes (Fig. 1), like mature neurons in the DG and OB (Wada et al. 1989; Le Jeune et al. 1995; Levey et al. 1995; Rouse et al. 1999; Quik et al. 2000). The immature neurons in the DG and OB are in contact with cholinergic fibers (Fig. 2), and are increased by ChEI-treatment (Figs 3–6). In contrast, the SVZ was found to be devoid of cholinergic innervation (Fig. 2) and insensitive to ChEI-treatment in our experiments (Figs 3 and 5). These results suggest that there is functional cholinergic transmission in the immature neurons in the DG and OB, which is involved in regulating adult neurogenesis.

Using PSA-NCAM as a marker for immature neurons and neuroblasts in combination with specific antibodies or ligands for various AChRs, we comprehensively studied the distributions of major AChRs in the DG and OB (Fig. 1). m1 and m4 were recently reported to be expressed by immature DG cells labeled with BrdU 24 h after injection (Mohapel et al. 2005). Consistently, a subpopulation of PSA-NCAM–positive cells in the DG was positive for m1 and m4 AChRs. Moreover, these cells also expressed nicotinic (α7 and β2) AChRs. We further demonstrated that PSA-NCAM–positive migrating neuroblasts in the OB similarly expressed several types of nicotinic and muscarinic receptors. These findings suggest that immature neurons can receive cholinergic stimulation directly. In fact, these AChR subtypes play roles in various regulatory processes for neural progenitor cells. α7, a major nAChR subunit most abundantly distributed in the DG (Seguela et al. 1993; Quik et al. 2000), is involved in neuroprotection against excitotoxic stimulation (Kihara et al. 1997; Shimohama et al. 1998; Prendergast et al. 2001) and participates in neurite outgrowth in olfactory cultures (Coronas et al. 2000), which is important for the survival of newborn neurons. In fact, previous studies have demonstrated several molecular mechanisms involving nicotine, via the α7 nicotinic receptor, which promote the survival of cultured neurons. Nicotine attenuates the expression of pro-apoptotic proteins such as caspase3, 8 and 9, and increases the levels of anti-apoptotic factors including phosphorylated Akt and Bcl-2 (Garrido et al. 2001; Kihara et al. 2001), possibly involved in the effect of ChEI in promoting the survival of newborn neurons as demonstrated in this study. Herein, α7nAChRs were detectable in almost all mature granule cells in both the OB and the DG. The proportion of α7-positive cells among PSA-NCAM-positive immature neurons was much lower in the OB (less than 20%) than that in the DG (over 70%), probably because most new neurons generated in the SVZ do not express α7 until they have differentiated into mature interneurons. Indeed, a previous study with retroviral labeling indicated that neuroblasts take about 1 week to reach the deeper GCL in the OB (Petreanu & Alvarez-Buylla 2002). Consistently, immature neurons in the OB showed delayed reactivity to ChEI-treatment as compared to those in the DG; 1 week treatment promoted the survival of newborn cells only in the DG, while longer treatment (for 4 weeks) affected both the DG and the OB. Previous reports indicate that AChRs are also involved in regulating cell-proliferation (Ma et al. 2000; Abrous et al. 2002; Jang et al. 2002), although we found no significant differences in the numbers of proliferating cells among our ChEI-treated animals. Thus, immature neurons express

multiple AChRs that have different effects on neurogenesis. ChEI-treatment increases the extracellular ACh concentration, which should stimulate all of the AChRs available on immature neurons and neuroblasts. Therefore, the results of ChEI-treatment experiments may reflect effects on multiple receptors with distinct functions expressed by immature neurons.

Our results indicate that chronic cholinergic stimulation with ChEI-treatment promotes the survival of newborn neurons in the DG and OB (Figs 4–6), but does not affect the proliferation of progenitor cells (Fig. 3). In contrast, acute treatment with another ChEI (physostigmine) was reported to increase cell proliferation, but not to affect the long-term survival of newborn cells in the DG (Mohapel et al. 2005). We used donepezil, a potent ChEI widely used for treatment of Alzheimer's disease, which has a longer-lasting action and greater specificity for acetylcholinesterase than any other ChEIs currently available, while exerting a minimal impact on the peripheral nervous system (Kosasa et al. 1999). These pharmacological properties make donepezil highly suitable for studying adult neurogenesis, considering that changes in physical conditions such as voluntary activity and nutrition reportedly modify neurogenesis (van Praag et al. 1999; Brown et al. 2003; Mattson et al. 2003). The difference in treatment duration may also account for the discrepancy between the results of these two studies. ChEI rapidly increases the extracellular ACh concentration, within several hours after a single administration (Kosasa et al. 1999). However, it often takes several months to exert clinical effects such as memory and cognitive improvement (Rogers et al. 1998). Although the precise mechanisms underlying this long-term effect of ChEIs have not been demonstrated, chronic ChEI-treatment up-regulates nicotinic AChRs and down-regulates muscarinic AChRs (Nilsson-Hakansson et al. 1990; Barnes et al. 2000), which is likely to result in changes in the amount and/or balance of signals mediated via each AChR. Thus, the protective effect of long-term ChEI-treatment on immature neurons observed in this study may be highly relevant to the clinical efficacy of ChEIs.

The extracellular ACh level in the brain varies depending on various changes which occur under physiological conditions. Learning, motor activity and estrogen treatment increase ACh release in the cortex and hippocampus (Day et al. 1991; Mizuno et al. 1991; Gabor et al. 2003). All of these conditions also promote the survival of new neurons and enhance neurogenesis in the DG and/or SVZ (Gould et al. 1999; van Praag et al. 1999; Banasr et al. 2001; Smith et al. 2001), suggesting the increased ACh level to be at least partially responsible for the increased neurogenesis. Conversely, selective

lesioning of the BFC system reduces neurogenesis in the adult rat brain (Calza et al. 2003; Cooper-Kuhn et al. 2004). Therefore, it is possible that the cholinergic system is among the physiologically important mechanisms regulating adult neurogenesis. Moreover, nAChRs in these regions are reduced in response to various insults including chronic stress, aging, traumatic injury and degenerative disorders such as Alzheimer's disease (Banerjee et al. 2000; Burghaus et al. 2000; Rei et al. 2000; Verbois et al. 2002, 2003; Gahring et al. 2005). BFC neurons are vulnerable to inflammatory processes induced by these lesions (Wenk et al. 2003). Thus, the cholinergic system can be impaired in various situations causing a decrease in neurogenesis. Therefore, increasing the ACh level using ChEI is likely to be a promising strategy for reversing the decrease in neurogenesis resulting from these insults. Indeed, our data indicate that an activated BFC system is capable of restoring neurogenesis in a restraint-induced stress model. ChEI-treatment improves the survival of newborn neurons in the DG and OB (Fig. 7). If the increased survival of newborn neurons results in functional recovery, ChEI-treatment may be useful for increasing neuronal plasticity and facilitating neuronal regeneration in injury/aging as well as under normal conditions.

Experimental procedures

Animals

ChEI-treatment

Donepezil (Aricept) was generously provided by Eisai Co., Ltd, Japan. Mice were intraperitoneally injected with saline (control, $n = 5$ or 6) or donepezil (0.5, 1 or 2 mg/weight (kg)/day, $n = 4$ or 5) for 1, 2 or 4 weeks consecutively (see Figs 3–5 for details).

Chronic stress protocol

Mice were separated into three groups. In the restraint group, mice were injected (i.p.) with either ChEI (donepezil 1.0 mg/weight (kg)/day, $n = 4$) or saline ($n = 5$) for 1 week, injected twice with bromodeoxyuridine (BrdU, Sigma, St. Louis, MO, USA) (50 mg/kg, i.p.) with a 2-h interval, and then placed in a close-fit cylindrical restrainer (acrylic tube 2.8 cm in diameter with ventilating holes on the top and bottom to avoid elevating

body temperature) inside their home cage for 6 h per day for 4 consecutive weeks. To decrease effects on the motor activities and food intakes of the mice, the restraint was performed during the light period, while the mice were inactive. ChEI or saline was injected immediately before each restraint period. Mice in the control group ($n = 5$) were treated with saline and BrdU for 1 week as described above, and then left undisturbed in their home cages for another 4 weeks. Before the final restraint, blood was sampled for measurement of the plasma corticosterone level using an enzyme immunoassay kit (Assay Designs, Ann Arbor, MI, USA).

BrdU labeling

To assess the effects of the donepezil treatments on cell-proliferation in the DG, SVZ, RMS and OB, mice were intraperitoneally injected with BrdU (50 mg/kg) immediately after 2 weeks of donepezil treatment, and allowed to survive for another 24 h before perfusion. To assess the differentiation and survival of the newborn cells, mice were injected with BrdU (50 mg/kg) twice with a 2-h interval at the beginning of the donepezil treatment or restraint stress exposure.

Immunohistochemistry

Mice were deeply anesthetized with diethyl ether and tran-scardially perfused with PBS, followed by 4% paraformaldehyde in 0.1 M phosphate buffer. The brains were removed and postfixed in the same fixative for 24 h at 4 °C. Fifty-micrometer serial sections were coronally cut on a vibratome (VT1000S, Leica, Heidelberg, Germany) and collected in PBS.

For AChR-immunostainings (Fig. 1), sections were incubated with antibodies against muscarinic AChR m1 (m1AChR, rabbit, 1 : 300, Sigma), m2 (m2AChR, rabbit, 1 : 300, Alomone labs, Israel) or m4 (m4AChR, rabbit, 1 : 300, Santa Cruz Biotechnology, Santa Cruz, CA, USA), or the β2 subunit of nicotinic AChR (β2nAChR, rabbit, 1 : 100, Santa Cruz) combined with antibodies against the highly polysialylated neural cell adhesion molecule (PSA-NCAM) or neuronal nuclei (NeuN), at 4 °C overnight. After washing with 0.1% TritonX-100 in PBS (PBS-T), the sections were incubated with biotinylated anti-rabbit IgG anti-body (goat, 1 : 500, Jackson) for 2 h, followed by signal amplifi-cation with the avidin-biotin-complex (ABC)-system (Vectastain ABC Elite kit, Vector Laboratories, Burlingame, CA, USA) for 1 h, and visualized with rhodamine-labeled thyramide (Perk-inElmer, Boston, MA, USA). The sections were then incubated in Alexa Fluor 488-conjugated anti-mouse IgM or IgG antibody (goat, 1 : 500, Molecular Probes) for 2 h. To detect α7nAChR, sections were incubated in rhodamine-conjugated α-bungarotoxin (α-BTX) for 2 h at 37 °C, followed by incubation in antibodies for PSA-NCAM or NeuN overnight at 4 °C. After washing, the sections were incubated with Alexa Fluor 488-conjugated anti-mouse IgM or IgG antibodies (goat, 1 : 500, Molecular Probes) mixed with Hoechst 333442 (Sigma) for 2 h.

For choline acetyltransferase (ChAT) immunohistochemistry (Fig. 2), sections were pretreated in cold (−20 °C) methanol for 6 min, and then boiled in 0.01 M citric acid (pH 6.0) for 30 s.

Following treatment with 1% H_2O_2 for 1 h, the sections were preincubated in TNB blocking reagent (PerkinElmer) for 2 h at room temperature, and incubated overnight in anti-ChAT antibody (goat, 1 : 100, Chemicon International, Temacula, CA, USA) mixed with anti-PSA-NCAM antibody (mouse, 1: 2000, kindly provided by Dr Tatsunori Seki) (Seki & Arai 1993) at 4 °C. After washing with PBS-T, sections were incubated with biotinylated anti-goat IgG (donkey, 1 : 500, Jackson Immuno Research Laboratories, West Grove, PA, USA) for 2 h. The ChAT signal was amplified using an ABC-system (Vector Laboratories) and visualized with fluorescein-labeled thyramide (TSA Fluorescence Systems, PerkinElmer). These sections were then incubated with Alexa Fluor 568-conjugated anti-mouse IgM or anti-mouse IgG antibody (goat, 1 : 500, Molecular Probes, the Netherlands), and Hoechst 33342 (Sigma) to stain the nuclei for 2 h at room temperature.

For BrdU staining (Figs 3–5), a series of floating sections, with 250-μm intervals, from each animal were incubated in 2 N HCl for 30 min at 60 °C, and then incubated with anti-BrdU antibody (mouse, 1 : 200, Becton Dickinson, Franklin Lakes NJ, USA) overnight at 4 °C. After washing with PBS-T, the sections were incubated in biotinylated anti-mouse IgG antibody (1 : 500, Jackson). The signal was visualized using an ABC Elite kit (Vector Laboratories) and diaminobenzidine (DAB).

For double-labeling with BrdU and NeuN (Figs 6 and 7), following the incubation in HCl, sections were incubated in antibodies for BrdU (rat, 1 : 200, Abcam Ltd, Cambridge, UK) and NeuN (mouse, 1 : 200, Chemicon) overnight at 4 °C, then incubated in biotinylated anti-rat IgG antibody (donkey, 1 : 500, Jackson) and finally Alexa Fluor 488-conjugated anti-mouse IgG antibody (goat, 1 : 500, Molecular Probes) for 2 h at room temperature. The BrdU signal was amplified with an ABC system, and visualized by rhodamine-labeled thyramide (PerkinElmer).

For Ki67 staining (Figs 5 and 7), sections were incubated in anti-Ki67 antibody (rabbit, 1 : 800, Novocastra, Newcastle, UK) overnight at 4 °C, and then in Alexa Fluor 488-conjugated anti-rabbit antibody (goat, 1 : 500, Molecular Probes) for 2 h.

Image processing and quantification

All the slides were coded before quantitative analysis, and the code was not broken until the analysis was complete. Cell counting was consistently performed by the same investigator (NK) blind to the group identification of each section. BrdU-labeled cells in the GCL and SGZ in the DG were counted under 400× magnifi-cation (Axioplan 2, Carl Zeiss, Germany). Cell numbers were counted using six or seven 50 μm-thick sections (250 μm apart) per animal. Therefore, the total number of cells in the DG was cal-culated by multipling the number of cells counted in these sections by six. For the SVZ, RMS and OB, absolute cell numbers were counted and presented. BrdU-labeled cells and Ki67 positive cells in the DG (SGZ and GCL), SVZ, RMS and OB were counted at 400× magnification under a microscope (Axioplan 2, Carl Zeiss, Germany). Pyknotic cells were identified and counted using DG and OB sections stained with Cresyl violet. The areas of the GCL and SGZ in each section were measured using Photoshop (Adobe) to calculate the density of pyknotic cells In the DG. BrdU-labeled

cells in the DG and five randomly chosen areas scanned in the OB were captured by confocal laser microscopy (Carl Zeiss, LSM510, C-apochromat 40×/1.20 W objective and C-apochromat 63×/1.20 W objective lenses) to confirm double-labeling with NeuN. Cells were considered double-labeled if colabeling was seen throughout the extent of the nucleus on 1 μm optical sections. Co-localizations of AChR signals with neuronal markers (PSA-NCAM and NeuN) were analyzed on 1.0 μm optical sections, and contacts of ChAT-positive cholinergic fibers on to PSA-NCAM-positive immature neurons were analyzed on 0.4 μm optical sections using confocal laser microscopy (LSM510; Carl Zeiss).

Statistical analysis

The obtained data were expressed as mean ± SE. Differences between means were determined by one-way ANOVA, followed by the Bonferroni post hoc multiple comparison test. Differences were regarded as statistically significant when $P < 0.05$.

Acknowledgements

References

Abrous, D.N., Adriani, W., Montaron, M.F., Aurousseau, C., Rougon, G., Le Moal, M. & Piazza, P.V. (2002) Nicotine self-administration impairs hippocampal plasticity. *J. Neurosci.* **22**, 3656–3662.

Altman, J. (1969) Autoradiographic and histological studies of postnatal neurogenesis. IV. Cell proliferation and migration in the anterior forebrain, with special reference to persisting neurogenesis in the olfactory bulb. *J. Comp. Neurol.* **137**, 433–457.

Banasr, M., Hery, M., Brezun, J.M. & Daszuta, A. (2001) Serotonin mediates oestrogen stimulation of cell proliferation in the adult dentate gyrus. *Eur. J. Neurosci.* **14**, 1417–1424.

Banerjee, C., Nyengaard, J.R., Wevers, A., de Vos, R.A., Jansen Steur, E.N., Lindstrom, J., Pilz, K., Nowacki, S., Bloch, W. & Schroder, H. (2000) Cellular expression of α7 nicotinic acetylcholine receptor protein in the temporal cortex in Alzheimer's and Parkinson's diseaseñña stereological approach. *Neurobiol. Dis.* **7**, 666–672.

Barnes, C.A., Meltzer, J., Houston, F., Orr, G., McGann, K. & Wenk, G.L. (2000) Chronic treatment of old rats with donepezil or galantamine: effects on memory, hippocampal plasticity and nicotinic receptors. *Neuroscience* **99**, 17–23.

Berger, F., Gage, F.H. & Vijayaraghavan, S. (1998) Nicotinic receptor-induced apoptotic cell death of hippocampal progenitor cells. *J. Neurosci.* **18**, 6871–6881.

Berchtold, N.C., Kesslak, J.P. & Cotman, C.W. (2002) Hippocampal brain-derived neurotrophic factor gene regulation by exercise and the medial septum. *J. Neurosci. Res.* **68**, 511–521.

Bodnoff, S.R., Humphreys, A.G., Lehman, J.C., Diamond, D.M., Rose, G.M. & Meaney, M.J. (1995) Enduring effects of chronic corticosterone treatment on spatial learning, synaptic plasticity, and hippocampal neuropathology in young and mid-aged rats. *J. Neurosci.* **15**, 61–69.

Bonfanti, L., Olive, S., Poulain, D.A. & Theodosis, D.T. (1992) Mapping of the distribution of polysialylated neural cell adhesion molecule throughout the central nervous system of the adult rat: an immunohistochemical study. *Neuroscience* **49**, 419–436.

Brown, J., Cooper-Kuhn, C.M., Kempermann, G., Van Praag, H., Winkler, J., Gage, F.H. & Kuhn, H.G. (2003) Enriched environment and physical activity stimulate hippocampal but not olfactory bulb neurogenesis. *Eur. J. Neurosci.* **17**, 2042–2046.

Burghaus, L., Schutz, U., Krempel, U., de Vos, R.A., Jansen Steur, E.N., Wevers, A., Lindstrom, J. & Schroder, H. (2000) Quantitative assessment of nicotinic acetylcholine receptor proteins in the cerebral cortex of Alzheimer patients. *Brain Res. Mol. Brain Res.* **76**, 385–388.

Calza, L., Giuliani, A., Fernandez, M., Pirondi, S., D'Intino, G., Aloe, L. & Giardino, L. (2003) Neural stem cells and cholinergic neurons: regulation by immunolesion and treatment with mitogens, retinoic acid, and nerve growth factor. *Proc. Natl. Acad. Sci. USA* **100**, 7325–7330.

Cameron, H.A., McEwen, B.S. & Gould, E. (1995) Regulation of adult neurogenesis by excitatory input and NMDA receptor activation in the dentate gyrus. *J. Neurosci.* **15**, 4687–4692.

Cameron, H.A., Woolley, C.S., McEwen, B.S. & Gould, E. (1993) Differentiation of newly born neurons and glia in the dentate gyrus of the adult rat. *Neuroscience* **56**, 337–344.

Caulfield, M.P. & Birdsall, N.J. (1998) International Union of Pharmacology. XVII. Classification of muscarinic acetylcholine receptors. *Pharmacol. Rev.* **50**, 279–290.

Changeux, J.P., Bertrand, D., Corringer, P.J., Dehaene, S., Edelstein, S., Lena, C., Le Novere, N., Marubio, L., Picciotto, M. & Zoli, M. (1998) Brain nicotinic receptors: structure and regulation, role in learning and reinforcement. *Brain Res. Brain Res. Rev.* **26**, 198–216.

Cooper-Kuhn, C.M., Winkler, J. & Kuhn, H.G. (2004) Decreased neurogenesis after cholinergic forebrain lesion in the adult rat. *J. Neurosci. Res.* **77**, 155–165.

Coronas, V., Durand, M., Chabot, J.G., Jourdan, F. & Quirion, R. (2000) Acetylcholine induces neuritic outgrowth in rat primary olfactory bulb cultures. *Neuroscience* **98**, 213–219.

Czeh, B., Welt, T., Fischer, A.K., Erhardt, A., Schmitt, W., Muller, M.B., Toschi, N., Fuchs, E. & Keck, M.E. (2002) Chronic psychosocial stress and concomitant repetitive transcranial magnetic stimulation: effects on stress hormone levels and adult hippocampal neurogenesis. *Biol. Psychiatry* **52**, 1057–1065.

Day, J., Damsma, G. & Fibiger, H.C. (1991) Cholinergic activity in the rat hippocampus, cortex and striatum correlates with

locomotor activity: an in vivo microdialysis study. *Pharmacol. Biochem. Behav.* **38**, 723–729.

Dayer, A.G., Ford, A.A., Cleaver, K.M., Yassaee, M. & Cameron, H.A. (2003) Short-term and long-term survival of new neurons in the rat dentate gyrus. *J. Comp. Neurol.* **460**, 563–572.

Doetsch, F. & Alvarez-Buylla, A. (1996) Network of tangential pathways for neuronal migration in adult mammalian brain. *Proc. Natl. Acad. Sci. USA* **93**, 14895–14900.

Eriksson, P.S., Perfilieva, E., Bjork-Eriksson, T., Alborn, A.M., Nordborg, C., Peterson, D.A. & Gage, F.H. (1998) Neurogenesis in the adult human hippocampus. *Nat. Med.* **4**, 1313–1317.

Fibiger, H.C. (1991) Cholinergic mechanisms in learning, memory and dementia: a review of recent evidence. *Trends Neurosci.* **14**, 220–223.

Frotscher, M. & Leranth, C. (1985) Cholinergic innervation of the rat hippocampus as revealed by choline acetyltransferase immunocytochemistry: a combined light and electron microscopic study. *J. Comp. Neurol.* **239**, 237–246.

Frotscher, M. & Leranth, C. (1986) The cholinergic innervation of the rat fascia dentata: identification of target structures on granule cells by combining choline acetyltransferase immunocytochemistry and Golgi impregnation. *J. Comp. Neurol.* **243**, 58–70.

Gabor, R., Nagle, R., Johnson, D.A. & Gibbs, R.B. (2003) Estrogen enhances potassium-stimulated acetylcholine release in the rat hippocampus. *Brain Res.* **962**, 244–247.

Gahring, L.C., Persiyanov, K., Days, E.L. & Rogers, S.W. (2005) Age-related loss of neuronal nicotinic receptor expression in the aging mouse hippocampus corresponds with cyclooxygenase-2 and PPAR gamma expression and is altered by long-term NS398 administration. *J. Neurobiol.* **62**, 453–468.

Garrido, R., Mattson, M.P., Hennig, B. & Toborek, M. (2001) Nicotine protects against arachidonic-acid-induced caspase activation, cytochrome c release and apoptosis of cultured spinal cord neurons. *J. Neurochem.* **76**, 1395–1403.

Gheusi, G., Cremer, H., McLean, H., Chazal, G., Vincent, J.D. & Lledo, P.M. (2000) Importance of newly generated neurons in the adult olfactory bulb for odor discrimination. *Proc. Natl. Acad. Sci. USA* **97**, 1823–1828.

Gould, E., Beylin, A., Tanapat, P., Reeves, A. & Shors, T.J. (1999) Learning enhances adult neurogenesis in the hippocampal formation. *Nat. Neurosci.* **2**, 260–265.

Gould, E., McEwen, B.S., Tanapat, P., Galea, L.A. & Fuchs, E. (1997) Neurogenesis in the dentate gyrus of the adult tree shrew is regulated by psychosocial stress and NMDA receptor activation. *J. Neurosci.* **17**, 2492–2498.

Han, J.S., Bizon, J.L., Chun, H.J., Maus, C.E. & Gallagher, M. (2002) Decreased glucocorticoid receptor mRNA and dysfunction of HPA axis in rats after removal of the cholinergic innervation to hippocampus. *Eur. J. Neurosci.* **16**, 1399–1404.

Harrist, A., Beech, R.D., King, S.L., Zanardi, A., Cleary, M.A., Caldarone, B.J., Eisch, A., Zoli, M. & Picciotto, M.R. (2004) Alteration of hippocampal cell proliferation in mice lacking the β2 subunit of the neuronal nicotinic acetylcholine receptor. *Synapse* **54**, 200–206.

Hefti, F. (1986) Nerve growth factor promotes survival of septal cholinergic neurons after fimbrial transections. *J. Neurosci.* **6**, 2155–2162.

Helm, K.A., Han, J.S. & Gallagher, M. (2002) Effects of cholinergic lesions produced by infusions of 192 IgG-saporin on glucocorticoid receptor mRNA expression in hippocampus and medial prefrontal cortex of the rat. *Neuroscience* **115**, 765–774.

Jang, M.H., Shin, M.C., Jung, S.B., Lee, T.H., Bahn, G.H., Kwon, Y.K., Kim, E.H. & Kim, C.J. (2002) Alcohol and nicotine reduce cell proliferation and enhance apoptosis in dentate gyrus. *Neuroreport* **13**, 1509–1513.

Kaplan, M.S. & Hinds, J.W. (1977) Neurogenesis in the adult rat: electron microscopic analysis of light radioautographs. *Science* **197**, 1092–1094.

Kihara, T., Shimohama, S., Sawada, H., Honda, K., Nakamizo, T., Shibasaki, H., Kume, T. & Akaike, A. (2001) α7 nicotinic receptor transduces signals to phosphatidylinositol 3-kinase to block A β-amyloid-induced neurotoxicity. *J. Biol. Chem.* **276**, 13541–13546.

Kihara, T., Shimohama, S., Sawada, H., Kimura, J., Kume, T., Kochiyama, H., Maeda, T. & Akaike, A. (1997) Nicotinic receptor stimulation protects neurons against β-amyloid toxicity. *Ann. Neurol.* **42**, 159–163.

Kosasa, T., Kuriya, Y., Matsui, K. & Yamanishi, Y. (1999) Effect of donepezil hydrochloride (E2020) on basal concentration of extracellular acetylcholine in the hippocampus of rats. *Eur. J. Pharmacol.* **380**, 101–107.

Le Jeune, H., Aubert, I., Jourdan, F. & Quirion, R. (1995) Comparative laminar distribution of various autoradiographic cholinergic markers in adult rat main olfactory bulb. *J. Chem. Neuroanat.* **9**, 99–112.

Leanza, G., Nilsson, O.G., Wiley, R.G. & Bjorklund, A. (1995) Selective lesioning of the basal forebrain cholinergic system by intraventricular 192 IgG-saporin: behavioural, biochemical and stereological studies in the rat. *Eur. J. Neurosci.* **7**, 329–343.

Lee, J., Duan, W. & Mattson, M.P. (2002) Evidence that brain-derived neurotrophic factor is required for basal neurogenesis and mediates, in part, the enhancement of neurogenesis by dietary restriction in the hippocampus of adult mice. *J. Neurochem.* **82**, 1367–1375.

Levey, A.I., Edmunds, S.M., Koliatsos, V., Wiley, R.G. & Heilman, C.J. (1995) Expression of m1–m4 muscarinic acetylcholine receptor proteins in rat hippocampus and regulation by cholinergic innervation. *J. Neurosci.* **15**, 4077–4092.

Luine, V., Villegas, M., Martinez, C. & McEwen, B.S. (1994) Repeated stress causes reversible impairments of spatial memory performance. *Brain Res.* **639**, 167–170.

Luskin, M.B. (1993) Restricted proliferation and migration of postnatally generated neurons derived from the forebrain subventricular zone. *Neuron* **11**, 173–189.

Ma, W., Maric, D., Li, B.S., Hu, Q., Andreadis, J.D., Grant, G.M., Liu, Q.Y., Shaffer, K.M., Chang, Y.H., Zhang, L., Pancrazio, J.J., Pant, H.C., Stenger, D.A. & Barker, J.L. (2000) Acetylcholine stimulates cortical precursor cell proliferation in vitro via muscarinic receptor activation and MAP kinase phosphorylation. *Eur. J. Neurosci.* **12**, 1227–1240.

Madsen, T.M., Kristjansen, P.E., Bolwig, T.G. & Wortwein, G. (2003) Arrested neuronal proliferation and impaired hippocampal function following fractionated brain irradiation in the adult rat. *Neuroscience* **119**, 635–642.

Mattson, M.P., Duan, W. & Guo, Z. (2003) Meal size and frequency affect neuronal plasticity and vulnerability to disease: cellular and molecular mechanisms. *J. Neurochem.* **84**, 417–431.

McGurk, S.R., Levin, E.D. & Butcher, L.L. (1991) Impairment of radial-arm maze performance in rats following lesions involving the cholinergic medial pathway: reversal by arecoline and differential effects of muscarinic and nicotinic antagonists. *Neuroscience* **44**, 137–147.

Mizuno, T., Endo, Y., Arita, J. & Kimura, F. (1991) Acetylcholine release in the rat hippocampus as measured by the microdialysis method correlates with motor activity and exhibits a diurnal variation. *Neuroscience* **44**, 607–612.

Mohapel, P., Leanza, G., Kokaia, M. & Lindvall, O. (2005) Forebrain acetylcholine regulates adult hippocampal neurogenesis and learning. *Neurobiol. Aging* **26**, 939–946.

Nilsson-Hakansson, L., Lai, Z. & Nordberg, A. (1990) Tetrahydroaminoacridine induces opposite changes in muscarinic and nicotinic receptors in rat brain. *Eur. J. Pharmacol.* **186**, 301–305.

Nishimura, J., Endo, Y. & Kimura, F. (1999) A long-term stress exposure impairs maze learning performance in rats. *Neurosci. Lett.* **273**, 125–128.

Petreanu, L. & Alvarez-Buylla, A. (2002) Maturation and death of adult-born olfactory bulb granule neurons: role of olfaction. *J. Neurosci.* **22**, 6106–6113.

Pham, K., Nacher, J., Hof, P.R. & McEwen, B.S. (2003) Repeated restraint stress suppresses neurogenesis and induces biphasic PSA-NCAM expression in the adult rat dentate gyrus. *Eur. J. Neurosci.* **17**, 879–886.

van Praag, H., Christie, B.R., Sejnowski, T.J. & Gage, F.H. (1999) Running enhances neurogenesis, learning, and long-term potentiation in mice. *Proc. Natl. Acad. Sci. USA* **96**, 13427–13431.

van Praag, H., Schinder, A.F., Christie, B.R., Toni, N., Palmer, T.D. & Gage, F.H. (2002) Functional neurogenesis in the adult hippocampus. *Nature* **415**, 1030–1034.

Prendergast, M.A., Harris, B.R., Mayer, S., Holley, R.C., Hauser, K.F. & Littleton, J.M. (2001) Chronic nicotine exposure reduces N-methyl-D-aspartate receptor-mediated damage in the hippocampus without altering calcium accumulation or extrusion: evidence of calbindin-D28K overexpression. *Neuroscience* **102**, 75–85.

Quik, M., Polonskaya, Y., Gillespie, A., Jakowec, M., Lloyd, G.K. & Langston, J.W. (2000) Localization of nicotinic receptor subunit mRNAs in monkey brain by in situ hybridization. *J. Comp. Neurol.* **425**, 58–69.

Ravel, N., Elaagouby, A. & Gervais, R. (1994) Scopolamine injection into the olfactory bulb impairs short-term olfactory memory in rats. *Behav. Neurosci.* **108**, 317–324.

Rei, R.T., Sabbagh, M.N., Corey-Bloom, J., Tiraboschi, P. & Thal, L.J. (2000) Nicotinic receptor losses in dementia with Lewy bodies: comparisons with Alzheimer's disease. *Neurobiol. Aging* **21**, 741–746.

Rochefort, C., Gheusi, G., Vincent, J.D. & Lledo, P.M. (2002) Enriched odor exposure increases the number of newborn neurons in the adult olfactory bulb and improves odor memory. *J. Neurosci.* **22**, 2679–2689.

Rogers, S.L., Farlow, M.R., Doody, R.S., Mohs, R. & Friedhoff, L.T. (1998) A 24-week, double-blind, placebo-controlled trial of donepezil in patients with Alzheimer's disease. Donepezil Study Group. *Neurology* **50**, 136–145.

Rogers, S.L. & Friedhoff, L.T. (1996) The efficacy and safety of donepezil in patients with Alzheimer's disease: results of a US multicentre, randomized, double-blind, placebo-controlled trial. The donepezil study group. *Dementia* **7**, 293–303.

Rouse, S.T., Marino, M.J., Potter, L.T., Conn, P.J. & Levey, A.I. (1999) Muscarinic receptor subtypes involved in hippocampal circuits. *Life Sci.* **64**, 501–509.

Seguela, P., Wadiche, J., Dineley-Miller, K., Dani, J.A. & Patrick, J.W. (1993) Molecular cloning, functional properties, and distribution of rat brain α7: a nicotinic cation channel highly permeable to calcium. *J. Neurosci.* **13**, 596–604.

Seki, T. & Arai, Y. (1993) Highly polysialylated neural cell adhesion molecule (NCAM-H) is expressed by newly generated granule cells in the dentate gyrus of the adult rat. *J. Neurosci.* **13**, 2351–2358.

Seki, T. & Arai, Y. (1995) Age-related production of new granule cells in the adult dentate gyrus. *Neuroreport* **6**, 2479–2482.

Shimohama, S., Greenwald, D.L., Shafron, D.H., Akaika, A., Maeda, T., Kaneko, S., Kimura, J., Simpkins, C.E., Day, A.L. & Meyer, E.M. (1998) Nicotinic α7 receptors protect against glutamate neurotoxicity and neuronal ischemic damage. *Brain Res.* **779**, 359–363.

Shors, T.J., Miesegaes, G., Beylin, A., Zhao, M., Rydel, T. & Gould, E. (2001) Neurogenesis in the adult is involved in the formation of trace memories. *Nature* **410**, 372–376.

Sithichoke, N. & Marotta, S.F. (1978) Cholinergic influences on hypothalamic-pituitary-adrenocortical activity of stressed rats: an approach utilizing agonists and antagonists. *Acta Endocrinol.* **89**, 726–736.

Smith, M.T., Pencea, V., Wang, Z., Luskin, M.B. & Insel, T.R. (2001) Increased number of BrdU-labeled neurons in the rostral migratory stream of the estrous prairie vole. *Horm. Behav.* **39**, 11–21.

Tanapat, P., Hastings, N.B., Rydel, T.A., Galea, L.A. & Gould, E. (2001) Exposure to fox odor inhibits cell proliferation in the hippocampus of adult rats via an adrenal hormone-dependent mechanism. *J. Comp. Neurol.* **437**, 496–504.

Verbois, S.L., Scheff, S.W. & Pauly, J.R. (2002) Time-dependent changes in rat brain cholinergic receptor expression after experimental brain injury. *J. Neurotrauma* **19**, 1569–1585.

Verbois, S.L., Hopkins, D.M, Scheff, S.W & Pauly, J.R. (2003) Chronic intermittant nicotine administration attenuates traumatic brain injury-induced cognitive dysfunction. *Neuroscience* **119**, 1199–1208.

Wada, E., Wada, K., Boulter, J., Deneris, E., Heinemann, S., Patrick, J. & Swanson, L.W. (1989) Distribution of α2, α3, α4, and β2 neuronal nicotinic receptor subunit mRNAs in the central nervous system: a hybridization histochemical study in the rat. *J. Comp. Neurol.* **284**, 314–335.

Wenk, G.L., McGann, K., Hauss-Wegrzyniak, B. & Rosi, S. (2003) The toxicity of tumor necrosis factor-α upon cholinergic neurons within the nucleus basalis and the role of norepinephrine in the regulation of inflammation: implications for Alzheimer's disease. *Neuroscience* **121**, 719–729.

Wenk, H., Meyer, U. & Bigl, V. (1977) Centrifugal cholinergic connections in the olfactory system of rats. *Neuroscience* **2**, 797–800.

Williams, L.R., Varon, S, Peterson, G.M., Wictorin, K, Fischer, W., Bjorklund, A. & Gage, F.H. (1986) Continuous infusion of nerve growth factor prevents basal forebrain neuronal death after

fimbria fornix transection. *Proc. Natl. Acad. Sci. USA* **83**, 9231–9235.

Zaborszky, L., Carlsen, J., Brashear, H.R. & Heimer, L. (1986) Cholinergic and GABAergic afferents to the olfactory bulb in the rat with special emphasis on the projection neurons in the nucleus of the horizontal limb of the diagonal band. *J. Comp. Neurol.* **243**, 488–509.

Zigova, T., Pencea, V., Wiegand, S.J. & Luskin, M.B. (1998) Intra-ventricular administration of BDNF increases the number of newly generated neurons in the adult olfactory bulb. *Mol. Cell. Neurosci.* **11**, 234–245.

Neuroprotective Effects of Angiotensin II Type 1 Receptor (AT1R) Blocker, Telmisartan, via Modulating AT1R and AT2R Signaling in Retinal Inflammation

Toshihide Kurihara,[1,2,3,4] *Yoko Ozawa,*[1,2,3,4] *Kei Shinoda,*[5] *Norihiro Nagai,*[1,3] *Makoto Inoue,*[1] *Yuichi Oike,*[3,6] *Kazuo Tsubota,*[1] *Susumu Ishida,*[1,3] *and Hideyuki Okano*[2]

PURPOSE. To investigate the retinal neural damage that occurs during inflammation and the therapeutic effects of the angiotensin II type 1 receptor (AT1R) blocker, telmisartan, using a model of endotoxin-induced uveitis (EIU).

METHODS. The localization of AT1R and AT2R was shown by immunohistochemistry. EIU was induced by intraperitoneal injection of lipopolysaccharide (LPS). Animals were treated with telmisartan for 2 days and were evaluated 24 hours later. Expression levels of angiotensin II, STAT3 activation induced by inflammatory cytokines, and retinal proteins essential for neural activities (e.g., synaptophysin, rhodopsin) were analyzed by immunoblot. An AT2R antagonist was administered to evaluate the contribution of AT2R signaling in this therapy. Dark-adapted full-field electroretinography (ERG) was also performed.

RESULTS. AT1R and AT2R were expressed in presynaptic terminals in most of the retinal neurons. AT1R was also expressed in Müller glial cells. During inflammation, angiotensin II expression was elevated, STAT3 was activated, and synaptophysin and rhodopsin expression were reduced. The expression of glial fibrillary acidic protein (GFAP), downstream of STAT3 activation, was induced in Müller glial cells. However, treatment with telmisartan successfully avoided all these changes. An AT2R antagonist lowered synaptophysin expression despite the treatment. STAT3 activity was negatively correlated with rhodopsin expression. Furthermore, ERG responses, which were mostly prevented by telmisartan, were disturbed during inflammation.

CONCLUSIONS. Retinal protein expression and visual function are both disturbed by inflammation. Treatment with the AT1R blocker telmisartan efficiently prevented these signs of retinal neural damage through the reduction of local angiotensin II expression, the blockade of AT1R, and the relative upregula-
tion of AT2R function. (*Invest Ophthalmol Vis Sci.* 2006;47: 5545–5552) DOI:10.1167/iovs.06-0478

Inflammatory reactions are involved in most retinal diseases, among them diabetic retinopathy and vascular occlusive diseases, leading to visual loss.[1,2] During inflammation, various kinds of cytokines, such as interleukin (IL)-6[3–5] and tumor necrosis factor (TNF)-α,[3] have been reported to cause pathologic changes. In addition to these cytokines, angiotensin II,[2,6–10] conventionally known as a regulator of salt and water retention and of systemic blood pressure, has received attention as a modulator of inflammation.[2,7,11] It is produced in many organs and in ocular tissue[8,9] from angiotensinogen through the renin/angiotensin system (RAS). Angiotensin II is highly expressed intraocularly in human diabetic retinopathy,[8–10,12] suggesting that it is involved in the retinal disease process.

We have already reported that angiotensin II causes pathologic changes in the retinal vascular system through the angiotensin II type 1 receptor (AT1R), which mainly mediates the angiotensin II signal.[2,13] On the other hand, AT1R signaling also affects neural synaptic activity in the brain.[14–17] Thus, angiotensin II may damage retinal neural cells during inflammation, but the exact influences of this signal and the effects of the AT1R blocker on retinal neural cells remain to be elucidated. Another angiotensin II receptor, AT2R, acts in a manner opposite that of AT1R signaling, especially under stress conditions, and possibly plays a role[15] in this therapy, but it also remains obscured.

In this study, we first described that AT1R and AT2R are expressed in most retinal neural cells, including synapses. Then we evaluated the influences of inflammation with excessive angiotensin II and the effects of treatment with telmisartan on retinal neural cells using animal model of lipopolysaccharide (LPS)-induced inflammation. This is also known as a model of endotoxin-induced uveitis (EIU) in which pan-retinal vasculitis occurs[2] and various kinds of cytokines, such as IL-6,[2,18] are induced. In addition, angiotensin II is upregulated in the retina, as we show in this study.

To evaluate retinal damage, we analyzed the retinal neural proteins synaptophysin and rhodopsin, which are essential for visual function. Synaptophysin is a presynaptic vesicle protein that controls neurotransmitter release. Rhodopsin is the major visual substance we have recently found to be negatively regulated by STAT3 activation in the neonatal retina.[19,20] Although AT1R is well known to be coupled with G-protein, it is also in the upstream of the JAK/STAT pathway.[21,22] Thus, we analyzed whether a similar response occurs in the adult retina. Given that excessive angiotensin II expressed during inflammation may selectively bind to AT2R after AT1R blockade, the contribution of AT2R signaling in this therapy is also evaluated by the administration of an AT2R-specific antagonist. Finally, we perform electroretinography (ERG), a common and objective clinical method for estimating visual function.

All our data show that AT1R, expressed in most of the retinal neural cells, plays key roles in retinal neural damage during inflammation. We have already reported the possibility of applying the AT1R blocker, telmisartan, in treating retinal vascular inflammation, and the present study demonstrates that it is also effective in protecting physical activities of the neural retina during inflammation.

Materials and Methods

Animals

C57BL/6 mice (8 weeks old) were purchased (Clea Japan, Tokyo, Japan). All animal experiments were conducted in accordance with the ARVO Statement for the Use of Animals in Ophthalmic and Vision Research. Each mouse received a single intraperitoneal injection of 6.0 mg/kg body weight of lipopolysaccharide (LPS) from *Escherichia coli* (Sigma, St. Louis, MO) in phosphate-buffered saline (PBS). Mice were killed and evaluated 24 hours after LPS injection. This time point was chosen for analysis because most of the pathologic changes in the retina were obvious by this time. Mice were treated with intraperitoneal injections of vehicle (0.25% dimethyl sulfoxide [DMSO] in PBS) or the AT1R blocker, telmisartan (120 μM in 0.25% DMSO, 20 mg/kg body weight; a gift of Boehringer Ingelheim, Ingelheim, Germany) on the day before and the day of the LPS injection. The AT2R blocker, PD123319[23] (10 mg/kg body weight; Tocris Cookson, Ltd., Bristol, UK) and the peroxisome proliferation–activated receptor γ (PPAR-γ) antagonist GW9662[24] (10 mg/kg body weight; Alexis Biochemicals, San Diego, CA) were intraperitoneally injected when telmisartan was injected.

Immunohistochemistry

Cryosections (14–16 μm) were prepared by perfusing mice with 4% paraformaldehyde (PFA), as described previously.[19] For immunostaining of rabbit anti–AT1R (1:100; Santa Cruz Biotechnology, Santa Cruz, CA), rabbit anti–AT2R (1:100, Santa Cruz Biotechnology), and mouse anti–synaptophysin (1:100 Sigma), sections were incubated with 1% H_2O_2 in PBS for 20 minutes and at 4°C overnight with the primary antibody diluted in blocking reagent with 0.1% Triton. The sections were then incubated with biotin-conjugated goat anti-rabbit IgG (1:500; Chemicon International, Temecula, CA) or biotin-conjugated goat anti-mouse IgG (1:500; Vector Laboratories, Burlingame, CA) and with a prepared avidin-biotin-peroxidase complex (Vectastain ABC Elite Kit; Vector Laboratories) and then were detected with a tyramide signaling amplification (TSA) fluorescein system (PerkinElmer Life Science, Boston, MA). For immunostaining of rabbit anti–glial fibrillary acidic protein (anti-GFAP, 1:1000; DAKO, Carpinteria, CA) and mouse anti-neurofilament (1:100, Roche), mouse anti–glutamine synthetase (1:400 Molecular Probes, Eugene, OR), sections were incubated and detected with Alexa 568-conjugated goat anti-rabbit, or Alexa 488–conjugated goat anti-mouse IgG (1:500; Molecular Probes), respectively. Nuclei were stained with the nuclear dye bisbenzimide 1:1000 from a stock solution of 10 mg/mL stain (Hoechst 33258; Sigma). Sections were examined with a laser scanning confocal microscope (LSM510; Carl Zeiss, Jena, Germany).

Immunoblot Analysis

Mice were killed with an overdose of anesthesia. The eyes were immediately enucleated, and the retina was carefully isolated and placed in lysis buffer. The lysate was separated with sodium dodecyl sulfate-polyacrylamide gel electrophoresis (SDS-PAGE) and electrophoretically transferred to polyvinylidene fluoride (PVDF) membrane (Millipore Corp., Bedford, MA). After blocking with 4% skim milk, the membranes were incubated overnight with rabbit anti-angiotensin II antibody (1:200; Peninsula Laboratories, Belmont, CA), rabbit anti–AT1R antibody (1:100; Santa Cruz Biotechnology), mouse anti-synaptophysin antibody (1:500; Sigma), rabbit anti-phosphorylated-STAT3

antibody (1:1000; Cell Signaling Technology, Beverly MA), rabbit anti-rhodopsin antibody (1:10,000; Cosmo Bio, Tokyo, Japan), and anti-α-tubulin (1:2000; Sigma) to equalize the amount of protein in each sample, respectively. Membranes were then incubated with biotin-conjugated secondary antibodies followed by avidin-biotin complex (Vectastain ABC Elite Kit; Vector Laboratories) or horseradish peroxidase–conjugated secondary antibodies. Finally, they were detected through enhanced chemiluminescence (ECL Blotting Analysis System; Amersham, Arlington Heights, IL) and measured by an NIH image. Statistic analysis was performed by the Bonferroni/Dunn test.

ERG

Mice were dark adapted for at least 12 hours and prepared under dim red illumination, anesthetized with 70 mg/kg body weight of pentobarbital sodium (Dainippon Sumitomo Pharmaceutical Co., Osaka, Japan). and placed on a heating pad throughout the experiment. The pupils were dilated with one drop of a mixture of 0.5% tropicamide and 0.5% of phenylephrine (Santen Pharmaceutical Co., Osaka, Japan). The ground electrode was a needle placed subcutaneously in the tail, and the reference electrode was placed subcutaneously between the eyes. The active electrodes were gold wires placed on the cornea. Recordings were performed (PowerLab System 2/25; AD Instruments, New South Wales, Australia). Responses were differentially amplified and filtered through a digital bandpass filter ranging from 0.313 to 1000 Hz to yield a- and b-waves. Light pulses of 800 cd $\cdot$ s/m² and 4-ms duration were delivered through a commercial stimulator (Ganzfeld System SG-2002; LKC Technologies, Inc., Gaithersburg, MD). Electrode impedance was checked before and after each measurement in all animals with the use of the machine's built-in feature. The implicit time of the a- and b-waves was measured from the onset of stimuli to the peak of each wave. Three researchers measured the amplitude of the a-wave from baseline to the trough of the a-wave and the amplitude of the b-wave from the trough of the a-wave to the peak of the b-wave. Statistical analysis was carried out with the Fisher PLSD test.

Results

Expression of AT1R and AT2R in the Retina

We first analyzed the expression of AT1R and AT2R in the retina of adult mice under physiological conditions. AT1R expression was observed in the inner plexiform layer (IPL), inner plexiform layer (OPL), and retinal ganglion cell layer (GCL; Fig. 1A). AT1R in the IPL and OPL was coexpressed with synaptophysin, a presynaptic vesicle membrane protein (Figs. 1B, 1C, insets), indicating that AT1R is expressed in synapses. This is consistent with previous reports that AT1R is expressed in the presynaptic terminals of the neurons, where it modulates the kinetics of the synaptic vesicles.[14–17,25] It includes synapses in the rod photoreceptor cells (B, arrows) judging from the localization. AT1R was also coexpressed with neurofilament (Fig. 1D) and was thus expressed in nerve fibers in the GCL and OPL. Moreover, it was coexpressed with glutamine synthetase (Fig. 1E), indicating that AT1R is also expressed in Müller glial cells. Some of the AT1R expression in the GCL seemed to be present in vascular endothelial cells, judging from its structure, as reported previously.[2]

AT2R, which is known to function in response to stress, was clearly expressed in the IPL and OPL under control conditions (Fig. 1F). Most of the AT2R was coexpressed with synaptophysin, indicating that AT2R is present in synaptic sites (Figs. 1G, 1H). The most intense staining for AT2R in the innermost IPL was double positive with anti-PKCα, one of the rod bipolar cell markers (data not shown). AT2R expression was also slightly observed in nerve fibers in the GCL.

Next we compared the expression levels of angiotensin II, AT1R, and AT2R in the retina during inflammation with or without treatment using telmisartan. Expression of angiotensin

FIGURE 1. Expression of AT1R and AT2R in the retinas of adult mice under control conditions. AT1R (A) was coexpressed with synaptophysin, a presynaptic vesicle protein, in the IPL and OPL (marked area in (A) was magnified in (B) and (C) and merged in (C)). Coexpression of AT1R (green) and synaptophysin (red) was clearly observed in the magnified images of the IPL and OPL (C, arrows in insets). AT1R was probably expressed in photoreceptor cells judging from the localization (B, arrows). AT1R was also coexpressed with neurofilament, a marker for nerve fibers in the GCL and OPL (D, arrows), and glutamine synthetase, a marker for Müller glial cells (E, arrows). AT2R was mainly expressed in the IPL and OPL (F), most of which were coexpressed with synaptophysin (marked area in (F) was magnified in (G) and (H) and merged in (H)). AT2R was probably expressed in photoreceptor cells (G, arrows). It was slightly observed in nerve fibers in the GCL (F). GCL, ganglion cell layer; IPL, inner plexiform layer; INL, inner nuclear layer; OPL, outer plexiform layer; ONL, outer nuclear layer; NF, neurofilament; GS, glutamine synthetase. Immunoblot analyses. Expression of angiotensin II (I, J) was upregulated by LPS injection and suppressed after treatment with telmisartan, though it remained at a level higher than control (Control: LPS/LPS + telmisartan; 1.00:2.68:1.88; n = 6:6:8; *P < 0.05; **P < 0.01; Bonferroni/Dunn test (I, J). Expression level of AT1R (Control: LPS/LPS + telmisartan; 1.00:2.15: 1.41; n = 6:6:8; **P < 0.05; Bonferroni/Dunn test (K, L)) was upregulated in LPS-induced inflammatory retina, whereas it was downregulated after treatment with telmisartan.
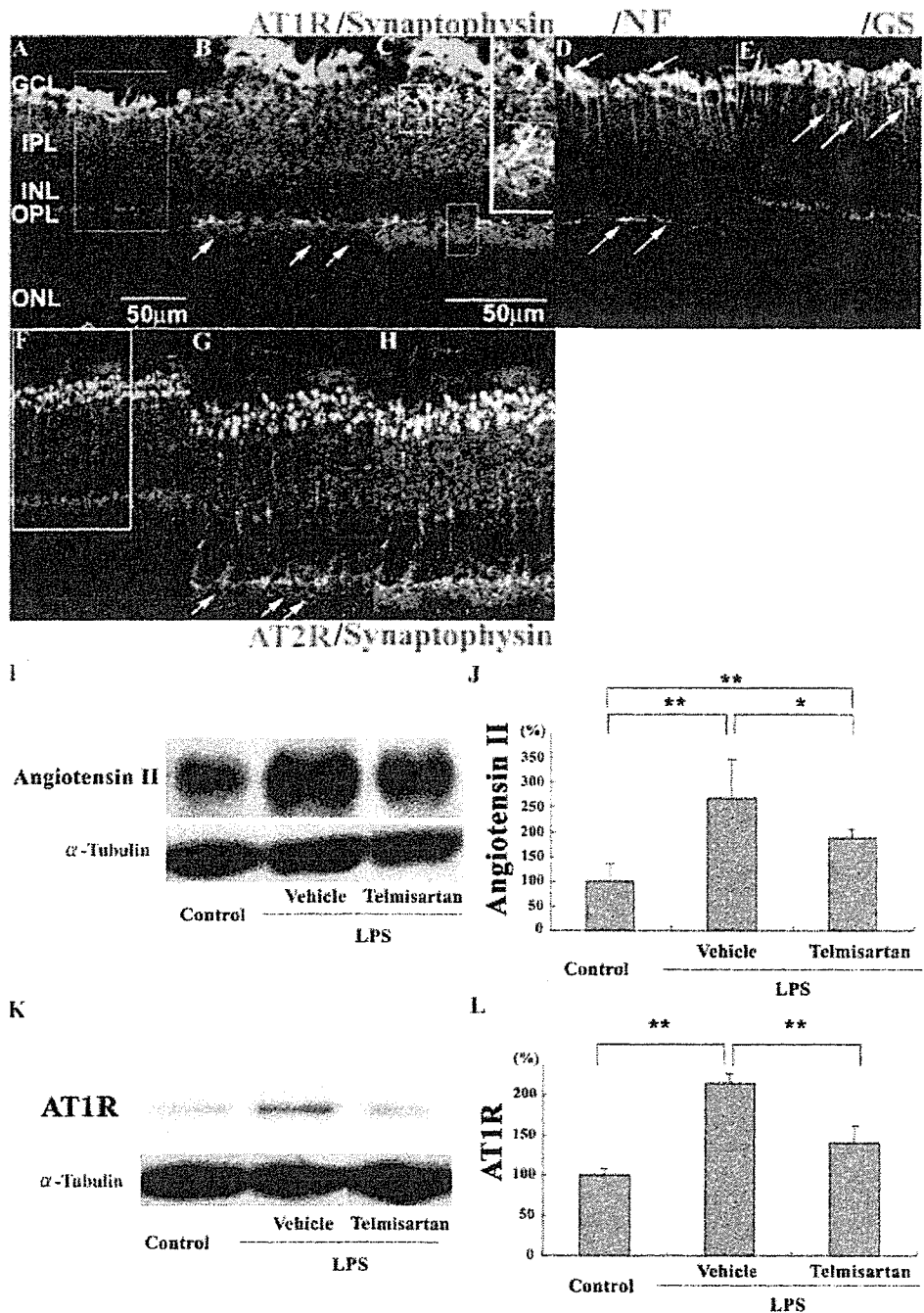
II was 2.7-fold upregulated by LPS injection, which was significantly suppressed by treatment with telmisartan, although it remained upregulated compared with control (control, LPS/LPS + telmisartan; 1.00:2.68:1.88; Figs. 1I, 1J).

AT1R expression was also upregulated during inflammation and was clearly suppressed by treatment with telmisartan (control, LPS/LPS + telmisartan; 1.00:2.15:1.41; Figs. 1K, 1L). This was consistent with the report in the brain[26,27] that AT1R expression is upregulated by a positive feedback system. Thus, the administration of AT1R blocker efficiently cut off the feedback loop. On the other hand, AT2R expression was 2.8-fold upregulated after LPS injection and was still maintained at a high level (2.3-fold) after treatment with telmisartan (data not shown).

Protective Effect of Telmisartan on Synaptophysin Expression during Inflammation

Both AT1R and AT2R were well expressed in synapses in the retina. To investigate the effect of angiotensin II on synapses, we analyzed the expression level of synaptophysin. The expression of synaptophysin during LPS-induced inflammation was significantly reduced, but it was clearly prevented by telmisartan. To evaluate the possible contribution of AT2R signaling in telmisartan treatment, we next injected an AT2R antagonist, PD123319, in addition to LPS and telmisartan. The expression of synaptophysin was lower after PD123319 injection even after LPS-induced inflammation was treated with telmisartan, though the level was clearly higher compared with

A

Synaptophysin

α-Tubulin

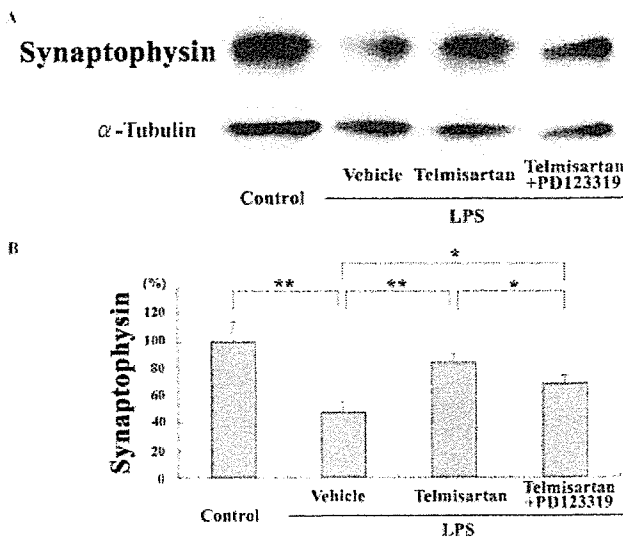| Control	Vehicle	Telmisartan	Telmisartan +PD123319
		LPS	

B

Figure 2. Reduction in synaptophysin expression during inflammation was prevented by telmisartan. Synaptophysin expression during retinal inflammation was significantly reduced, but telmisartan clearly prevented the change. Restored synaptophysin expression by telmisartan was partially cancelled after administration of the AT2R antagonist PD123319 (Control: LPS/LPS + telmisartan/LPS + telmisartan + PD123319; 1:0.48:0.85:0.69; n = 6:5:5:5; $**P$ < 0.01; $*P$ < 0.05; Bonferroni/Dunn test (A, B)).

the LPS-induced inflammatory retina with no treatment (control, LPS/LPS + telmisartan/LPS + telmisartan + PD123319; 1:0.48:0.85:0.69; n = 6:5:5:5; $**P$ < 0.01; $*P$ < 0.05; Bonferroni/Dunn test; Figs. 2A, 2B). This suggested that the upregulation of AT2R function relative to AT1R was involved in rescuing the expression of synaptophysin in this therapy.

Given that additional partial PPAR-γ agonist activity is spontaneously found in telmisartan,[28,29] its contribution was also analyzed by administration of the PPAR-γ antagonist, GW9662, in addition to telmisartan. Although a high dose of GW9662 was injected compared with previous reports,[24,30,31] the level of synaptophysin expression was not changed (data not shown), suggesting that there was less contribution of PPAR-γ activity in this case.

Thus, the AT1R blocker telmisartan inhibited the reduction of synaptophysin expression during retinal inflammation, by the blockade of AT1R and the relative upregulation of AT2R function.

Protective Effect of Telmisartan on Rhodopsin Expression during Inflammation with Reduction of Activated STAT3

After LPS injection, the expression of angiotensin II was upregulated (Figs. 1I, 1J), and in its downstream, the inflammatory cytokine IL-6[2,32] was induced, as we have previously reported.[2] Both ligands can activate STAT3,[33] which causes multiple events, depending on the cell type. Immunoblot analysis showed that STAT3 was highly activated in the neural retina but that it was significantly prevented by telmisartan (control, LPS/LPS + telmisartan; 1.00:1.92:1.51; Figs. 3A, 3B). Although AT2R[21] and PPAR-γ[34] activity has been reported to inhibit STAT3 activation biochemically, neither receptor activity showed any contribution (data not shown). Therefore, strong STAT3 activation was induced by retinal inflammation but was prevented by AT1R blockade.

Next, we analyzed whether rhodopsin expression negatively correlated with STAT3 activation, as it did in the neonatal

retina. During inflammation with intense STAT3 activation, rhodopsin expression was significantly downregulated toward 40% of the control condition. However, treatment with telmisartan, which avoided excessive STAT3 activation, successfully preserved rhodopsin expression (control, LPS/LPS + telmisartan; 1.0:0.40:0.91; Figs. 3C, 3D). Because immunohistochemical findings showed that the number of photoreceptor cells was not altered and that TUNEL-positive cells were rarely observed in this model (data not shown), each rod photoreceptor cell might have reduced the level of rhodopsin expression. The contribution of AT2R function or PPAR-γ activity was not observed (data not shown). Thus, rhodopsin expression was attenuated during inflammation and negatively correlated with strong STAT3 activation, which was efficiently prevented by AT1R blockade.

In the retina, Müller glial cells maintain the microenvironment, but, when pathologic events occur, they alter their characteristics to become reactive glial cells. It is recognized by GFAP upregulation,[35] which is induced by STAT3 activation.[35-37] Under control conditions, GFAP expression (Fig. 4A) in Müller glial cells (Fig. 4D) was only observed in their endfeet but was clearly induced through the columnar cell bodies when inflammation occurred (Figs. 4B, 4E). However, this was mostly avoided by treatment with telmisartan (Figs. 4C, 4F). These results suggested that STAT3 was also activated in Müller glial cells through the AT1R pathway.

Protective Effect of Telmisartan on Visual Responses after Retinal Inflammation

We next recorded full-field ERG after 12 hours of dark adaptation (Figs. 5A-E). Overall responses were reduced after inflammation but preserved by treatment with telmisartan. Amplitude of the a-wave was significantly lowered (control, LPS/LPS + telmisartan; 311:159:282 (μV); Figs. 5A, 5B), and the implicit time of the b-wave was prolonged (control, LPS/LPS + telmisartan; 44.7:83.5:65.3 (ms); Figs. 5A, 5E) after inflammation, but those changes were not observed after treatment with telmisartan. Therefore, functional analysis also showed that visual function was successfully rescued from retinal damage during inflammation by the AT1R blocker telmisartan.
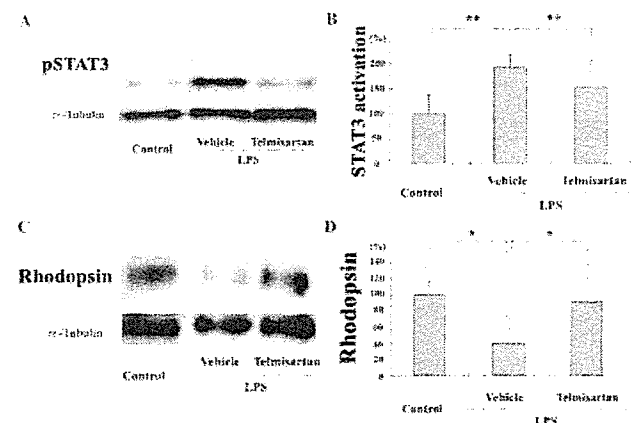
A   pSTAT3

B

C   Rhodopsin

D

Figure 3. Induction of STAT3 activation and reduction of rhodopsin expression during inflammation were effectively blocked by telmisartan. STAT3 activation induced during inflammation was inhibited by telmisartan (Control: LPS/LPS + telmisartan; 1.00:1.92:1.51; n = 6:6:7; $**P$ < 0.01; Bonferroni/Dunn test (A, B)). Rhodopsin expression was significantly suppressed during inflammation, which was clearly avoided by treatment with telmisartan (Control: LPS/LPS + telmisartan; 1.00:0.402:0.906; n = 6:7:9; $*P$ < 0.05; Bonferroni/Dunn test (C, D)).

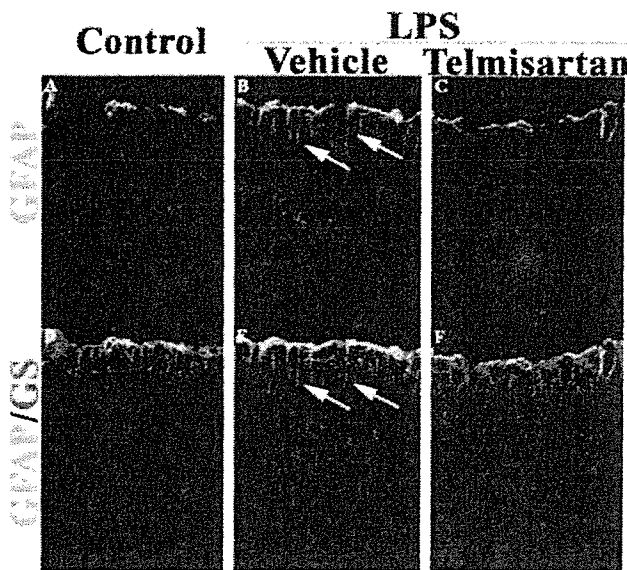**Control**

LPS

Vehicle **Telmisartan**

FIGURE 4. GFAP expression during inflammation was suppressed by telmisartan. GFAP expression (A–C) in Müller glial cells (D–F, detected by GS) was only observed in their endfeet in control conditions (A, D), but it was clearly upregulated through the columnar cell bodies during inflammation (B, E), which was observed less often after treatment with telmisartan (C, F). GFAP, glial fibrillary acidic protein; GS, glutamine synthetase.

DISCUSSION

We demonstrated that intense inflammation caused local upregulation of angiotensin II expression and thereby reduced the expression levels of rhodopsin and synaptophysin. We also showed severe disturbance of visual function by ERG. Treatment with the AT1R blocker telmisartan effectively prevented pathologic changes through the reduction of local angiotensin II expression, blockade of AT1R signaling with or without subsequent activation of STAT3, and relative upregulation of AT2R function. Both AT1R and AT2R are expressed in most of the retinal neural cells (Fig. 1), suggesting the possibility that telmisartan directly affects retinal neural cells.

High levels of angiotensin II were observed in the retina of this model with retinal inflammation. It is generally agreed that continuous activation of local RAS causes tissue inflammation rather than circulating angiotensin II.[9,38,39] This is also the case in the retina, and all the components for RAS are inducible in the neural retina or surrounding tissues.[8,9,10,12,40,41] In particular, the first substrate of RAS, angiotensinogen, is expressed in Müller glial cells[9,40] and is upregulated by STAT3 activation.[42,43] As shown in this study, STAT3 should be activated in Müller glial cells at least through AT1R during inflammation; thus, a high level of angiotensinogen may be induced during retinal inflammation. In addition, the expression of AT1R itself was also increased so that once triggered, angiotensin II could be produced continuously through AT1R in the retina. Thus, local angiotensin II expression in retinal tissue was efficiently inhibited by AT1R blockade in Müller glial cells. Therefore, one of the therapeutic targets for the AT1R blocker during retinal inflammation included reduction in local angiotensin II expression by cutoff of the positive feedback loop of locally activated RAS (Fig. 6).

Several changes were observed in retinal neurons and Müller glial cells under high levels of angiotensin II during inflammation that also appeared to be good therapeutic targets for the AT1R blocker telmisartan (Fig. 6).

The most obvious effect during inflammation was the reduction of rhodopsin expression, which should have disturbed the function of rod photoreceptor cells but was mostly prevented by treatment with the AT1R blocker telmisartan. The level of rhodopsin expression was negatively correlated with STAT3 activation, as in the neonatal retina.[19,20] Although rod photoreceptor cells express several kinds of cytokine receptors that can activate STAT3, STAT3 activation in photoreceptor cells is rarely observed under normal conditions.[19,20] In the
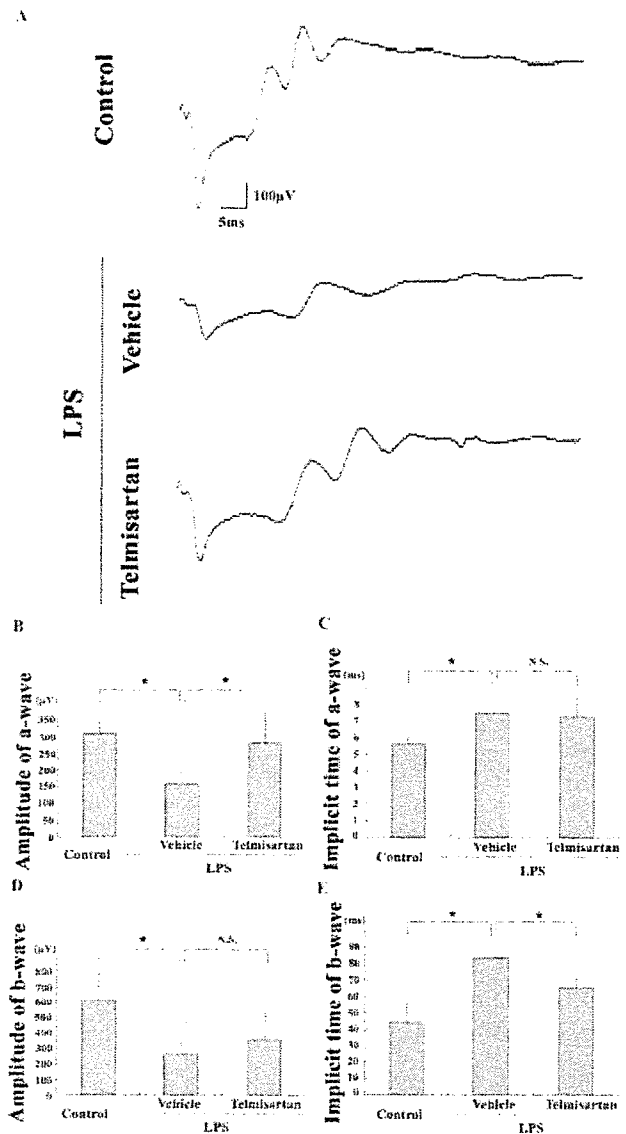

FIGURE 5. Abnormalities in ERG response during inflammation were markedly prevented by telmisartan. Full-field electroretinography (ERG) after 12 hours of dark adaptation (A). Overall responses were reduced in LPS-induced inflammatory retina but were mostly preserved after treatment with telmisartan. Amplitude and implicit time of a- and b-waves were significantly altered during inflammation and, notably, were saved by treatment. Amplitude of a-wave; control: LPS/LPS + telmisartan; 311:159:282 (μV); $n = 4:3:4$; *$P < 0.05$, Fisher PLSD test (B). Implicit time of a-wave; control: LPS/LPS + telmisartan; 5.63:7.45: 7.23 (ms); $n = 4:3:4$; *$P < 0.05$, Fisher PLSD test (C). Amplitude of b-wave; control: LPS/LPS + telmisartan; 616:267:361 (μV); $n = 4:3:4$; *$P < 0.05$, Fisher PLSD test (D). Implicit time of b-wave; control: LPS/LPS + telmisartan; 44.7:83.5:65.3 (ms); $n = 4:3:4$; *$P < 0.05$, Fisher PLSD test (E).
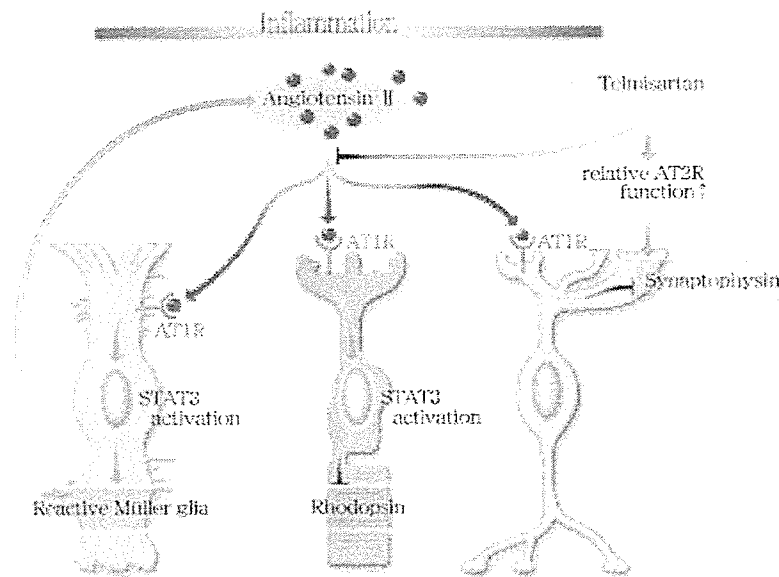
FIGURE 6. Model of mechanisms affecting retinal neural activities by angiotensin II during inflammation and therapeutic targets of telmisartan. Angiotensin II is highly upregulated during inflammation and dominantly binds to AT1R in the retinal neural cells. Through AT1R, STAT3 activation is induced in the Müller glial cells, upregulating GFAP expression and further increasing angiotensin II production. Thus, this inflammatory reaction is accelerated in a positive feedback manner. AT1R signaling also induces STAT3 activation in the rod photoreceptor cells, reducing rhodopsin expression. AT1R signaling downregulates synaptophysin expression in the retinal neurons. AT1R blockade with telmisartan successfully prevents these signs of retinal neural damage. In addition, the relative upregulation of AT2R function after AT1R blockade also contributes to the preservation of synaptophysin expression.

present study, however, the excessive stimuli should have activated STAT3 in the photoreceptor cells under pathologic conditions, as follows: AT1R signaling induces IL-6 expression in the retina[2] through NF-κB, and, in turn, IL-6 upregulates AT1R expression.[44] Both angiotensin II and IL-6 can activate STAT3; thus, excessive ligands should have forced STAT3 to activate synergistically in rod photoreceptor cells, which disturbs rhodopsin expression in adults. Conversely, the AT1R blocker suppressed the expression of these ligands and directly blocked AT1R, thus avoiding STAT3 activation in rod photoreceptor cells and reduction in rhodopsin expression.

Furthermore, synaptophysin expression during inflammation was reduced, which should have affected synaptic function by disturbing the exo-endocytosis of the synaptic vesicle essential for releasing neurotransmitters.[45] However, it was also averted by the AT1R blocker, telmisartan. Although AT2R was already expressed in synapses and has a level of affinity to angiotensin II almost identical with that of AT1R,[15] AT2R signaling could not eliminate the pathologic changes caused by AT1R signaling without treatment with the AT1R blocker, possibly because the expression level of AT2R was basically lower than that of AT1R. However, AT1R blockade probably led to the selective binding of angiotensin II to AT2R instead of AT1R. Moreover, the expression level of AT2R was not downregulated by AT1R blocker, which was advantageous for this therapy.

The mechanisms to rescue synaptophysin expression may be through direct AT1R signaling because AT1R signaling has been reported to control the kinetics of synaptic vesicles[25] and the expression of their components,[15] which can be cancelled by AT2R signaling.[46] Excessive AT1R signaling may promote the exocytosis of synaptic vesicles beyond the capacity of the re-uptake system to exhaust synaptophysin or to suppress the expression.

Abnormalities in Müller glial cells were also observed during inflammation. AT1R signaling promoted GFAP expression representing reactive Müller glial cells. The possible changes in reactive Müller glial cells included decreased uptake of glutamate[47,48] and GABA,[47,49] and they induced gliogenetic changes in the cells themselves afterward.[50] The accumulation of glutamate has been shown by clinical data in diabetic retinopathy.[47] These abnormalities might have affected the microenvironment of surrounding retinal neurons that indirectly altered their status.

Moreover, the changes in ERG responses were obvious. Telmisartan successfully preserved retinal function. Thus, AT1R signaling was responsible for disturbing visual function. The change in rhodopsin expression might have been involved in a-wave changes, and the malfunction of postsynaptic neural activity in INL cells or Müller glial cells might have been reflected in b-wave responses in ERG, though several other factors might also have been involved. These results further encourage us to use this therapy for patients with inflammatory diseases.

We demonstrated that local angiotensin II expression was extremely elevated during retinal inflammation, thereby influencing the condition of the retinal neural cells through AT1R signaling, which is expressed in most of the retinal cells. These changes were accelerated by positive feedback regulation through AT1R. Thus, telmisartan was effective for keeping the retinal neural cells from losing their physiological activities and normal ERG responses. We concluded that telmisartan plays key roles in neuroprotection and that it preserves good visual function by reducing inflammatory reactions in the retinal neural cells.

Acknowledgments

References

1. Joussen AM, Murata T, Tsujikawa A, Kirchhof B, Bursell SE, Adamis AP. Leukocyte-mediated endothelial cell injury and death in the diabetic retina. *Am J Pathol.* 2001;158:147–152.
2. Nagai N, Oike Y, Noda K, et al. Suppression of ocular inflammation in endotoxin-induced uveitis by blocking the angiotensin II type 1 receptor. *Invest Ophthalmol Vis Sci.* 2005;46:2925–2931.
3. de Vos AF, van Haren MA, Verhagen C, Hoekzema R, Kijlstra A. Kinetics of intraocular tumor necrosis factor and interleukin-6 in endotoxin-induced uveitis in the rat. *Invest Ophthalmol Vis Sci.* 1994;35:1100–1106.
4. Kramer M, Goldenberg-Cohen N, Axer-Siegel R, Weinberger D, Cohen Y, Monselise Y. Inflammatory reaction in acute retinal artery occlusion: cytokine levels in aqueous humor and serum. *Ocul Immunol Inflamm.* 2005;13:305–310.
5. Noma H, Funatsu H, Yamasaki M, et al. Pathogenesis of macular edema with branch retinal vein occlusion and intraocular levels of vascular endothelial growth factor and interleukin-6. *Am J Ophthalmol.* 2005;140:256–261.
6. Satofuka S, Ichihara A, Nagai N, et al. Suppression of ocular inflammation in endotoxin-induced uveitis by inhibiting nonproteolytic activation of prorenin. *Invest Ophthalmol Vis Sci.* 2006;47:2686–2692
7. Suzuki Y, Ruiz-Ortega M, Lorenzo O, Ruperez M, Esteban V, Egido J. Inflammation and angiotensin II. *Int J Biochem Cell Biol.* 2003;35:881–900.
8. Wilkinson-Berka JL. Angiotensin and diabetic retinopathy. *Int J Biochem Cell Biol.* 2006;38:752–765.
9. Berka JL, Stubbs AJ, Wang DZ, et al. Renin-containing Muller cells of the retina display endocrine features. *Invest Ophthalmol Vis Sci.* 1995;36:1450–1458.
10. Danser AH, van den Dorpel MA, Deinum J, et al. Renin, prorenin, and immunoreactive renin in vitreous fluid from eyes with and without diabetic retinopathy. *J Clin Endocrinol Metab.* 1989;68:160–167.
11. Das UN. Angiotensin-II behaves as an endogenous pro-inflammatory molecule. *J Assoc Physicians India.* 2005;53:472–476.
12. Danser AH, Derkx FH, Admiraal PJ, Deinum J, de Jong PT, Schalekamp MA. Angiotensin levels in the eye. *Invest Ophthalmol Vis Sci.* 1994;35:1008–1018.
13. Saavedra JM. Brain angiotensin II: new developments, unanswered questions and therapeutic opportunities. *Cell Mol Neurobiol.* 2005;25:485–512.
14. Sun C, Li H, Leng L, Raizada MK, Bucala R, Sumners C. Macrophage migration inhibitory factor: an intracellular inhibitor of angiotensin II-induced increases in neuronal activity. *J Neurosci.* 2004;24:9944–9952.
15. Gallinat S, Busche S, Yang H, Raizada MK, Sumners C. Gene expression profiling of rat brain neurons reveals angiotensin II-induced regulation of calmodulin and synapsin, I: possible role in neuromodulation. *Endocrinology.* 2001;142:1009–1016.
16. Dendorfer A, Thornagel A, Raasch W, Grisk O, Tempel K, Dominiak P. Angiotensin II induces catecholamine release by direct ganglionic excitation. *Hypertension.* 2002;40:348–354.
17. Li DP, Chen SR, Pan HL. Angiotensin II stimulates spinally projecting paraventricular neurons through presynaptic disinhibition. *J Neurosci.* 2003;23:5041–5049.
18. Hoekzema R, Verhagen C, van Haren M, Kijlstra A. Endotoxin-induced uveitis in the rat: the significance of intraocular interleukin-6. *Invest Ophthalmol Vis Sci.* 1992;33:532–539.
19. Ozawa Y, Nakao K, Shimazaki T, et al. Downregulation of STAT3 activation is required for presumptive rod photoreceptor cells to differentiate in the postnatal retina. *Mol Cell Neurosci.* 2004;26:258–270.
20. Rhee KD, Goureau O, Chen S, Yang XJ. Cytokine-induced activation of signal transducer and activator of transcription in photore-

ceptor precursors regulates rod differentiation in the developing mouse retina. *J Neurosci.* 2004;24:9779–9788.
21. Horiuchi M, Hayashida W, Akishita M, et al. Stimulation of different subtypes of angiotensin II receptors, AT1 and AT2 receptors, regulates STAT activation by negative crosstalk. *Circ Res.* 1999;84:876–882.
22. Touyz RM, Berry C. Recent advances in angiotensin II signaling. *Braz J Med Biol Res.* 2002;35:1001–1015.
23. Bivalacqua TJ, Dalal A, Lambert DG, Champion HC, Kadowitz PJ. Effects of candesartan and PD123319 on responses to angiotensin II in the anesthetized mouse. *J Am Soc Nephrol.* 1999;10(suppl 11):S98–S100.
24. Takagi T, Naito Y, Ichikawa H, et al. A PPAR-gamma ligand, 15-deoxy-Delta12,14-prostaglandin J(2), inhibited gastric mucosal injury induced by ischemia-reperfusion in rats. *Redox Rep.* 2004;9:376–381.
25. Sumners C, Fleegal MA, Zhu M. Angiotensin AT1 receptor signalling pathways in neurons. *Clin Exp Pharmacol Physiol.* 2002;29:483–490.
26. Barth SW, Gerstberger R. Differential regulation of angiotensinogen and AT1A receptor mRNA within the rat subfornical organ during dehydration. *Brain Res Mol Brain Res.* 1999;64:151–164.
27. Mascareno E, Siddiqui MA. The role of Jak/STAT signaling in heart tissue renin-angiotensin system. *Mol Cell Biochem.* 2000;212:171–175.
28. Benson SC, Pershadsingh HA, Ho CI, et al. Identification of telmisartan as a unique angiotensin II receptor antagonist with selective PPARgamma-modulating activity. *Hypertension.* 2004;43:993–1002.
29. Tuck ML. Angiotensin-receptor blocking agents and the peroxisome proliferator-activated receptor-gamma system. *Curr Hypertens Rep.* 2005;7:240–243.
30. Sivarajah A, McDonald MC, Thiemermann C. The cardioprotective effects of preconditioning with endotoxin, but not ischemia, are abolished by a peroxisome proliferator-activated receptor-gamma antagonist. *J Pharmacol Exp Ther.* 2005;313:896–901.
31. Collino M, Patel NS, Lawrence KM, et al. The selective PPAR-gamma antagonist GW9662 reverses the protection of LPS in a model of renal ischemia-reperfusion. *Kidney Int.* 2005;68:529–536.
32. Han Y, Runge MS, Brasier AR. Angiotensin II induces interleukin-6 transcription in vascular smooth muscle cells through pleiotropic activation of nuclear factor-kappa B transcription factors. *Circ Res.* 1999;84:695–703.
33. Bhat GJ, Thekkumkara TJ, Thomas WG, Conrad KM, Baker KM. Activation of the STAT pathway by angiotensin II in T3CHO/AT1A cells: cross-talk between angiotensin II and interleukin-6 nuclear signaling. *J Biol Chem.* 1995;270:19059–19065.
34. Kim HJ, Rho YH, Choi SJ, et al. 15-Deoxy-delta12,14-PGJ2 inhibits IL-6-induced Stat3 phosphorylation in lymphocytes. *Exp Mol Med.* 2005;37:179–185.
35. Peterson WM, Wang Q, Tzekova R, Wiegand SJ. Ciliary neurotrophic factor and stress stimuli activate the Jak-STAT pathway in retinal neurons and glia. *J Neurosci.* 2000;20:4081–4090.
36. Kahn MA, Huang CJ, Caruso A, et al. Ciliary neurotrophic factor activates JAK/Stat signal transduction cascade and induces transcriptional expression of glial fibrillary acidic protein in glial cells. *J Neurochem.* 1997;68:1413–1423.
37. Sun Y, Nadal-Vicens M, Misono S, et al. Neurogenin promotes neurogenesis and inhibits glial differentiation by independent mechanisms. *Cell.* 2001;104:365–376.
38. Hunyady L, Catt KJ. Pleiotropic AT1 receptor signaling pathways mediating physiological and pathogenic actions of angiotensin II. *Mol Endocrinol.* 2006;20:953–970.
39. Wilkinson-Berka JL, Fletcher EL. Angiotensin and bradykinin: targets for the treatment of vascular and neuro-glial pathology in diabetic retinopathy. *Curr Pharm Des.* 2004;10:3313–3330.
40. Wagner J, Jan Danser AH, Derkx FH, et al. Demonstration of renin mRNA, angiotensinogen mRNA, and angiotensin converting enzyme mRNA expression in the human eye: evidence for an intraocular renin-angiotensin system. *Br J Ophthalmol.* 1996;80:159–163.

41. Deinum J, Derkx FH, Danser AH, Schalekamp MA. Identification and quantification of renin and prorenin in the bovine eye. *Endocrinology*. 1990;126:1673–1682.

42. Mascareno E, Dhar M, Siddiqui MA. Signal transduction and activator of transcription (STAT) protein-dependent activation of angiotensinogen promoter: a cellular signal for hypertrophy in cardiac muscle. *Proc Natl Acad Sci USA*. 1998;95:5590–5594.

43. Fukuzawa J, Booz GW, Hunt RA, et al. Cardiotrophin-1 increases angiotensinogen mRNA in rat cardiac myocytes through STAT3: an autocrine loop for hypertrophy. *Hypertension*. 2000;35:1191–1196.

44. Wassmann S, Stumpf M, Strehlow K, et al. Interleukin-6 induces oxidative stress and endothelial dysfunction by overexpression of the angiotensin II type 1 receptor. *Circ Res*. 2004;94:534–541.

45. Valtorta F, Pennuto M, Bonanomi D, Benfenati F. Synaptophysin: leading actor or walk-on role in synaptic vesicle exocytosis? *Bioessays*. 2004;26:445–453.

46. Inagami T, Eguchi S, Numaguchi K, et al. Cross-talk between angiotensin II receptors and the tyrosine kinases and phosphatases. *J Am Soc Nephrol*. 1999;10(suppl 11:S57–S61.

47. Ambati J, Chalam KV, Chawla DK, et al. Elevated gamma-aminobutyric acid, glutamate, and vascular endothelial growth factor levels in the vitreous of patients with proliferative diabetic retinopathy. *Arch Ophthalmol*. 1997;115:1161–1166.

48. Li Q, Puro DG. Diabetes-induced dysfunction of the glutamate transporter in retinal Muller cells. *Invest Ophthalmol Vis Sci*. 2002;43:3109–3116.

49. Ishikawa A, Ishiguro S, Tamai M. Accumulation of gamma-aminobutyric acid in diabetic rat retinal Muller cells evidenced by electron microscopic immunocytochemistry. *Curr Eye Res*. 1996;15:958–964.

50. Lewis GP, Fisher SK. Up-regulation of glial fibrillary acidic protein in response to retinal injury: its potential role in glial remodeling and a comparison to vimentin expression. *Int Rev Cytol*. 2003;230:263–290.

Isolation of Multipotent Neural Crest-Derived Stem Cells from the Adult Mouse Cornea

SATORU YOSHIDA,[a,b] SHIGETO SHIMMURA,[a,b] NARIHITO NAGOSHI,[c] KEIICHI FUKUDA,[d] YUMI MATSUZAKI,[c] HIDEYUKI OKANO,[c] KAZUO TSUBOTA[a,b]

[a]Cornea Center, Tokyo Dental College, Ichikawa, Chiba, Japan; [b]Department of Ophthalmology, Keio University School of Medicine, Shinjuku-ku, Tokyo, Japan; [c]Department of Physiology, Keio University School of Medicine, Shinjuku-ku, Tokyo, Japan; [d]Department of Regenerative Medicine and Advanced Cardiac Therapeutics, Keio University School of Medicine, Shinjuku-ku, Tokyo, Japan

ABSTRACT

We report the presence of neural crest-derived corneal precursors (COPs) that initiate spheres by clonal expansion from a single cell. COPs expressed the stem cell markers *nestin, Notch1, Musashi-1,* and *ABCG2* and showed the side population cell phenotype. COPs were multipotent with the ability to differentiate into adipocytes, chondrocytes, as well as neural cells, as shown by the expression of β-III-tubulin, glial fibrillary acidic protein, and neurofilament-M. COP spheres prepared from E/nestin-enhanced green fluorescent protein (EGFP) mice showed induction of EGFP expression that was not originally observed in the cornea, indicating activation of the neural-specific nestin second intronic enhancer in culture.

COPs were Sca-1$^+$, CD34$^+$, CD45$^-$, and c-kit$^-$. Numerous GFP$^+$ cells were observed in the corneas of mice transplanted with whole bone marrow of transgenic mice ubiquitously expressing GFP; however, no GFP$^+$ COP spheres were initiated from these mice. On the other hand, COP spheres from transgenic mice encoding P0-Cre/Floxed-EGFP as well as Wnt1-Cre/Floxed-EGFP were GFP$^+$, indicating the neural crest origin of COPs, which was confirmed by the expression of the embryonic neural crest markers *Twist, Snail, Slug,* and *Sox9*. Taken together, these data indicate the existence of neural crest-derived, multipotent stem cells in the adult cornea. STEM CELLS 2006;24:2714–2722

INTRODUCTION

The cornea is an avascular, structurally unique tissue that functions as the primary refracting medium of the eye. Although anatomically continuous with the vascularized sclera and conjunctiva, all three major components of the cornea function together to maintain optically clear tissue. Therefore, homeostasis of the corneal epithelium, stroma, and endothelium—the cellular components of the cornea—is vital in preserving transparency and optical precision.

Stem cell researchers of the cornea have identified the epithelial stem cell to be located in the vascular rim, or limbus, of the cornea [1]. In contrast, there is little evidence of the existence of stem/progenitor cells for keratocytes [2, 3], the resident cells of the corneal stroma. Keratocytes, mesenchymal cells distinct from keratinocytes of the skin, repopulate corneal stroma during tissue remodeling after its depletion due

to disease, such as herpes simplex virus infection, and trauma [4, 5]. Although the stroma of the cornea develops from the cranial neural crest [6, 7], the origin of keratocytes involved in the turnover of stromal tissue is unknown.

We have previously demonstrated that the neurosphere culture technique, which was originally developed for neural stem cells (NSCs) isolated from the forebrain of mouse [8], can be adapted to culture mouse cornea stromal cells for more than 15 passages while still maintaining the keratocyte phenotype [9]. A recent report demonstrated that multipotent precursor cells from adult mouse and human dermis, termed skin-derived precursor cells (SKPs), also form spheres and differentiate into neural and mesenchymal cells [10–12]. We therefore hypothesized that the corneal stroma-derived spheres we have isolated also include putative keratocyte precursor cells similar to SKPs of the skin.

Table 1. Polymerase chain reaction primers

Gene		Primer sequence (5'-3')	Product size (bp)	GenBank accession ID
Abcg2	Forward:	CCATAGCCACAGGCCAAAGT	327	NM_011920
	Reverse:	GGGCCACATGATTCTTCCAC		
Nestin	Forward:	AATGGGAGGATGGAGAATGGAC	496	NM_016701
	Reverse:	TAGACAGGCAGGGCTAAGCAAG		
Musashi1	Forward:	GGCTTCGTCACTTTCATGGACC	542	NM_008629
	Reverse:	GGGAACTGGTAGGTGTAACCAG		
Notch1	Forward:	TGCCTGTGCACACCATCCTGC	247	NM_008714
	Reverse:	CAATCAGAGATGTTGGAATGC		
Twist	Forward:	CCAGAGAAGGAGAAAATGGACAGTC	259	NM_011658
	Reverse:	AAAAAGTGGGGTGGGGGGACACAAAC		
Snail	Forward:	CCCACTCGGATGTGAAGAGATACC	534	NM_011427
	Reverse:	ATGTGTCCAGTAACCACCCTGCTG		
Slug	Forward:	CACACACACACACACACACACAG	570	NM_011415
	Reverse:	TGTCTTTCCCTCCTCTTCCAAGG		
Sox9	Forward:	CGCCCATCACCCGCTCGCAATACG	545	NM_011448
	Reverse:	AAGCCCCTCCTCGCTGATACTGG		
Mpz	Forward:	TTCCTGCTCTCCCTTTCCTACC	422	NM_008623
	Reverse:	CCTTTCCTTCCCATTCTCGC		
Gapd	Forward:	GACCACAGTCCATGCCATCAC	453	NM_008084
	Reverse:	TCCACCACCCTGTTGCTGTAG		

Here, we show the existence of multipotent keratocyte precursor cells (termed COPs, for cornea-derived precursors) in cornea stromal spheres isolated from adult mice. Single cells dissociated from spheres initiated clonal growth of progeny spheres, and a subset of COPs exhibited the side population (SP) cell phenotype. We sought to determine whether COPs were of bone marrow (BM) origin or of neural crest lineage by initiating COP spheres in various transgenic mice.

MATERIALS AND METHODS

Animals

Normal, specific pathogen-free, adult C57BL/6J mice were purchased from CLEA Japan, Inc., Tokyo, http://www.clea-japan.com/index.html). Green fluorescent protein (GFP) transgenic mice (C57BL/6 TgN [act-enhanced GFP (EGFP)] OsbC14-Y01-FM131) were obtained from the Genome Information Research Center (Osaka University, Osaka, http://www.gen-info.osaka-u.ac.jp/welcome_en.html). Transgenic mice expressing Cre recombinase under the control of the Wnt1 promoter/enhancer (Wnt1-Cre mice) [13] and P0 promoter (P0-Cre mice) [14] were mated to CAG-CAT$^{loxP/loxP}$-EGFP (CAG-CAT-EGFP) transgenic mice [15] to obtain Wnt1-Cre/CAG-CAT-EGFP (Wnt1-Cre/Floxed-EGFP) and P0-Cre/CAG-CAT-EGFP (P0-Cre/Floxed-EGFP) transgenic mice, respectively. P0-Cre transgenic mice and CAG-CAT$^{loxP/loxP}$-EGFP transgenic mice were obtained from Dr. Ken-ichi Yamamura and Dr. Jun-ichi Miyazaki, respectively. All animal procedures were performed in accordance with institutional guidelines.

Cell Culture

Cells were dissociated from adult C57BL6/J mice and then cultured as described previously [9]. All animals were handled in full accordance with the ARVO (Association for Research in Vision and Ophthalmology) Statement for the Use of Animals in Ophthalmic and Vision Research. In brief, corneal stromal discs were cut into small pieces and digested in 0.05% trypsin (Sigma-Aldrich, St.

Louis, http://www.sigmaaldrich.com) for 30 minutes at 37°C, followed by 78 U/ml collagenase (Sigma-Aldrich) and 38 U/ml hyaluronidase (Sigma-Aldrich) treatment for 30 minutes at 37°C. Stromal cells were mechanically dissociated into single cells and cultured in Dulbecco's modified Eagle's medium (DMEM)/F-12 (1:1) supplemented with 20 ng/ml epidermal growth factor (EGF) (Sigma-Aldrich), 10 ng/ml fibroblastic growth factor 2 (FGF2) (Sigma-Aldrich), B27 supplement (Invitrogen, Carlsbad, CA, http://www.invitrogen.com), and 10^3 U/ml leukemia inhibitory factor (Chemicon International, Temecula, CA, http://www.chemicon.com) at a density of 1×10^5 cells per milliliter at 37°C, 5% CO_2.

For clonal sphere expansion, COPs were initiated from corneas of wild-type C57BL/6 strain and transgenic strain expressing GFP ubiquitously [16]. Cells dissociated from COPs were plated on six-well dishes at a cell density of 5×10^3 cells per milliliter and cultured for 6–7 days in DMEM/F-12 containing 0.8% methylcellulose with EGF, FGF2, and B27 supplement. The use of methyl cellulose in the clone culture of NSCs (neural spheres) is an established method reported by several groups [17–24].

To examine the expression of nestin in COPs, cells were prepared from transgenic mice carrying EGFP (Clontech, Mountain View, CA, http://www.clontech.com) under the control of the second intronic enhancer of the nestin gene, which acts selectively in neural stem/precursor cells (E/nestin-EGFP) [25]. To confirm the neural crest origin of COPs, corneal stromal cells were prepared from six corneas of neonatal (13 days) and three corneas of adult (8 weeks) P0-Cre/Floxed-EGFP mice, as well as from one cornea of an adult (10 weeks) Wnt1-Cre/Floxed-EGFP mouse and cultured as described above.

In Vitro Differentiation

To examine neural differentiation, COPs were dissociated into single cells and suspended at a cell density of 10 cells per milliliter. One-hundred microliters of the cell suspension was divided into 48-well culture plates, and only clonal spheres from single cells were subcultured and expanded. Clonal COPs were

plated and cultured on poly(L-ornithine)/laminin-coated Lab-Tek chamber slides (Nalge Nunc International, Rochester, NY, http://www.nalgenunc.com). For α-smooth muscle actin (α-SMA) expression, clonal cells were also plated on Lab-Tek chamber slides in transforming growth factor (TGF)-β-containing medium. For adipogenic or chondrogenic differentiation, dissociated COPs were cultured in differentiation-inducing medium (Cambrex Bio Science Walkersville, Inc., Walkersville, MD, http://www.cambrex.com) according to instructions provided by the manufacturer. To visualize adipogenic differentiation, cells were stained with oil red O (Sigma-Aldrich). Chondrogenic differentiation was observed by the expression of the specific markers collagen II and aggrecan analyzed by immunocytochemistry of cell pellets (see above). Results were expressed as mean ± SD.

Immunohistochemistry

Cultured cells and frozen-tissue sections were fixed with 4% paraformaldehyde (PFA) for 10 minutes at room temperature and then stained with the following antibodies: anti-Bcrp1 (1:250; R&D Systems, Minneapolis, http://www.rndsystems.com), anti-α-SMA (1:200; NeoMarkers, Fremont, CA, http://www.labvision.com), anti-collagen type II (1:40; Chemicon International), anti-aggrecan (1:40; Chemicon International), anti-Musashi-1 (Msi1) (1:500, clone 14H1) [26], anti-class III β-tubulin (1:100, R&D Systems), anti-glial fibrillary acidic protein (GFAP) (1:200; Chemicon International), and anti-neurofilament-M (NF-M) (1:500; Abcam, Cambridge, U.K., http://www.abcam.com). Immunohistochemistry for GFP was performed using an anti-GFP antibody (1:500; MBL, Nagoya, Japan, http://www.mbl.co.jp) in 10-μm frozen sections from eyes fixed in 2% PFA overnight at 4°C. Immunoreactivity of primary antibodies was visualized using secondary antibodies conjugated with fluorescein isothiocyanate or cyanine 3 (Jackson ImmunoResearch Laboratories, West Grove, PA, http://www.jacksonimmuno.com).

Reverse Transcription-Polymerase Chain Reaction

COPs and cells freshly dissociated from mouse corneal stroma were collected and immediately frozen in liquid N_2. cDNA was synthesized using a commercially available kit (Life Sciences, Inc., St. Petersburg, FL, http://www.lifesci.com) from total RNA prepared using RNeasy kit (Qiagen, Hilden, Germany, http://www1.qiagen.com). Primers used for Abcg2, Notch1, nestin, Msi1, Twist, Snail, Slug, Sox9, and Gapd are shown in Table 1 (supplemental online data). Polymerase chain reaction (PCR) was performed using GeneAmp 9700 (Applied Biosystems, Foster City, CA, http://www.appliedbiosystems.com).

Flow Cytometry

For Hoechst dye efflux assays, single cells dissociated from COP spheres were incubated with Hoechst 33342 dye (Dojindo Laboratories, Kumamoto, Japan, http://www.dojindo.com) for 60 minutes at 37°C in the presence or absence of 50 μM reserpine (Daiichi Pharmaceutical, Tokyo, http://www.daiichius.com). SP cells were gated using FACS Vantage (BD Biosciences Immunocytometry Systems, San Jose, CA, http://www.bdbiosciences.com) as described previously [27]. Surface marker expression was also analyzed by flow cytometry using antibodies for CD45, CD34, Sca-1,

c-kit, and CD133 (eBioscience, San Diego, http://www.ebioscience.com). Isotype-matched immunoglobulin G was used as negative control.

BM Transplantation

Whole BM (WBM) cells (1 × 10⁶ cells) were prepared from GFP-transgenic mice [16] and transplanted into the retro-orbital space of C57BL6/J recipient mice treated with a lethal dose (10.3 Gy) of irradiation. Eight weeks after transplantation, recipient mice were sacrificed, and corneal stromal cells were prepared for sphere culture. Cells from the transplanted animals and nonirradiated animals were then mixed and cultured as described above to assess WBM-derived cell contribution to COP sphere formation.

RESULTS

COPs Initiate Clonal Sphere Formation

Mouse corneal stromal-derived spheres were first prepared and cultured as described previously [9]. To determine whether spheres arise from single putative COPs or from aggregates of floating cells, we first performed the clonal sphere-forming assay [17]. As shown in Figure 1, homogeneous GFP-positive or -negative spheres were found 6 days after plating. More than 70% of spheres were homogenous; however, nonclonal spheres composed of GFP-positive and -negative cells were also observed. The same observation was made by Kawase et al. [17], who reported that SKPs may aggregate at an initial cell density of 1 × 10³ cells per milliliter during sphere cultures. Clonal sphere formation was observed for several passages (P5), suggesting that COPs possess high "self-renewing" potential.
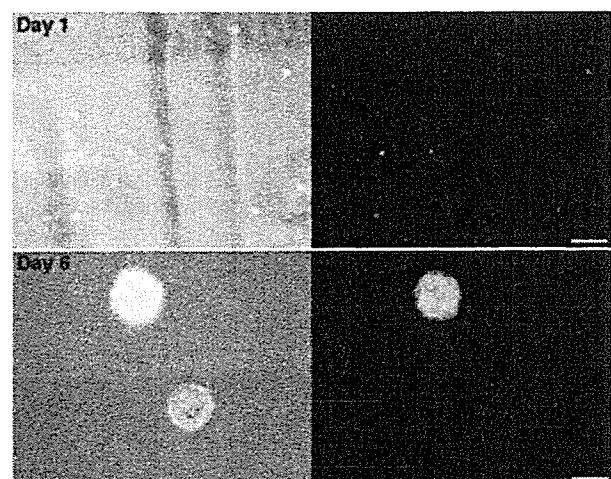

Figure 1. Single cornea-derived precursors form clonal spheres. Green fluorescent protein (GFP)-positive and -negative cells were mixed and cultured in methylcellulose-containing medium at a cell density of 5 × 10³ cells per milliliter. Right and left panels show fluorescent images and phase-contrast images merged with fluorescent images, respectively. Upper panels show images of the cells 1 day after plating. After 6 days of culture, clonal spheres that consist entirely of GFP-positive or -negative cells were observed (lower panels). Scale bars = 200 μm (upper panel) and 100 μm (lower panel).
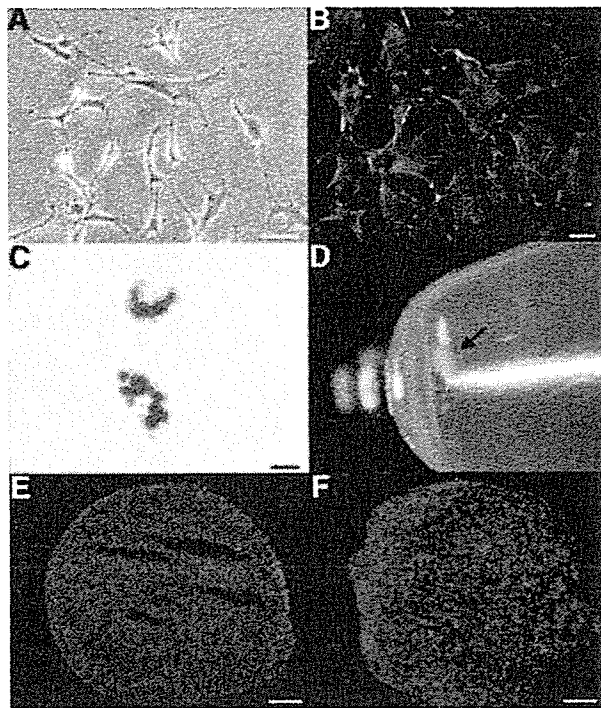
Figure 2. Cornea-derived precursors differentiate into mesenchymal cells. (A): Keratocyte phenotype in serum-free culture. (B): Anti-α-smooth muscle actin staining of myofibroblasts induced by transforming growth factor (TGF)-β. (C): Adipogenic cells stained with oil red O. Cells cultured in medium containing TGF-β3 formed chondrogenic pellets (D) (arrow) expressing collagen II (E) and aggrecan (F). Scale bars = 50 μm (A), 20 μm (B, C), and 100 μm (E, F).

Figure 3. COP spheres express neural stem/precursor and differentiation markers. (A): Reverse transcription-polymerase chain reaction analysis of neural stem cell markers *Notch1*, *Musashi1*, and *nestin* expressed in COPs. *Gapd* was loaded as an internal control. (B): Fluorescent image merged with transmitted-light image of a COP sphere prepared from an E/nestin-EGFP mouse. EGFP expression confirms the activation of neuronal nestin. (C): Immunocytochemical analysis showed high levels of Musashi-1 expressed in COP spheres. Differentiated cells from COP spheres express the neuronal markers GFAP (D), class III-β-tubulin (E), and NF-M (F). Cells were counterstained with 4,6-diamidino-2-phenylindole (blue) to show nuclei. Scale bars = 20 μm (B, C) and 50 μm (D–F). Abbreviations: COP, cornea-derived precursor; EGFP, enhanced green fluorescent protein; GFAP, glial fibrillary acidic protein; NF-M, neurofilament-M; RT, reverse transcription.

COPs Differentiate into Neural and Mesenchymal Lineage Cells

COPs differentiate into keratocytes when cultured on plastic (Fig. 2A), into fibroblasts when cultured with serum, and into myofibroblasts under TGF-β stimulation (Fig. 2B) [9]. To determine whether these cells possess the ability to differentiate into other cells of mesenchymal lineage, COPs were cultured in various differentiation-inducing media. After 10 days of culture in medium containing insulin, approximately 7.9% (mean, $n = 2$) of the cells differentiated into oil red O-positive lipid-producing adipocytes (Fig. 2C). In addition, cell pellets were formed when cells were cultured in chondrogenic-inducing medium containing TGF-β3 ($n = 9$) (Fig. 2D). Immunofluorescent staining showed expression of the chondrocyte markers, type II collagen and aggrecan [28] in the pellets (Fig. 2E, 2F).

The NSC marker *Msi1*, an RNA-binding protein involved in the maintenance of NSCs and activation of Notch signaling [26, 29, 30], was expressed in COP spheres (Fig. 3A, 3C). COP spheres also expressed the NSC markers *nestin* [25, 31] and *Notch1* (Fig. 3A); the latter is a gene involved in the self-renewal of various types of tissue stem cells, including NSCs [32]. Because Nestin is an intermediate filament expressed by several cell types [33], COP spheres were prepared from E/nestin-EGFP transgenic mice, which carry the EGFP transgene under the control of a NSC-selective en-
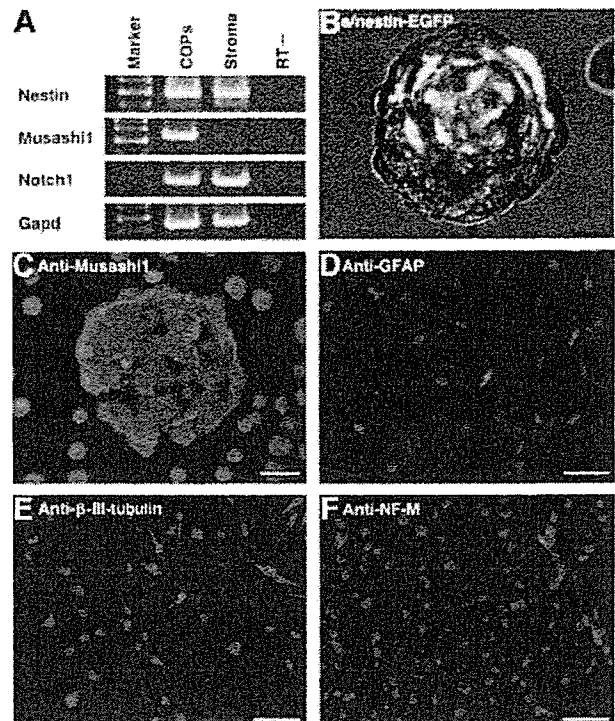
hancer [25]. As expected, EGFP-positive spheres were formed (Fig. 3B) from these mice, which originally did not show EGFP-related fluorescence in the cornea.

Neural differentiation of COPs was shown by the expression of class III β-tubulin, GFAP, and NF-M in cells cultured on poly(L-ornithine)-coated slides in differentiation-inducing medium (Fig. 3E, 3F). Approximately 1.4% of cells stained with anti-NF-M antibody ($n = 3$), 36.9% ± 17.7% expressed GFAP ($n = 3$), and 32.8% ± 15.8% expressed β-III-tubulin ($n = 3$).

COP Spheres Are Rich in SP Cells

Several studies have shown that the ability to exclude Hoechst dye is a property of stem cells commonly referred to as SP cells [34], which are distinguished from the "main population" by flow cytometric analysis. The SP cell phenotype is defined by the dye exclusion ability of an ABC transporter, ABCG2, which is inhibited by ABC-transporter inhibitors such as reserpine. We found that COP spheres expressed ABCG2 when examined by reverse transcription (RT)-PCR and immunocytochemistry (Fig.